

1 **The SCF^{Met30} ubiquitin ligase senses cellular redox state to regulate the**
2 **transcription of sulfur metabolism genes**

3

4 Zane Johnson¹, Yun Wang¹, Benjamin M. Sutter¹, Benjamin P. Tu^{1*}

5

6 ¹ Department of Biochemistry, University of Texas Southwestern Medical Center,
7 Dallas, TX 75390-9038

8

9 *Correspondence and Lead Contact: benjamin.tu@utsouthwestern.edu

10

11

12

13 SUMMARY

14
15 In yeast, control of sulfur amino acid metabolism relies upon Met4, a transcription factor which
16 activates the expression of a network of enzymes responsible for the biosynthesis of cysteine and
17 methionine. In times of sulfur abundance, the activity of Met4 is repressed via ubiquitination by
18 the SCF^{Met30} E3 ubiquitin ligase, but the mechanism by which the F-box protein Met30 senses
19 sulfur status to tune its E3 ligase activity remains unresolved. Here, using a combination of
20 genetics and biochemistry, we show that Met30 utilizes exquisitely redox-sensitive cysteine
21 residues in its WD-40 repeat region to sense the availability of sulfur metabolites in the cell.
22 Oxidation of these cysteine residues in response to sulfur starvation inhibits binding and
23 ubiquitination of Met4, leading to induction of sulfur metabolism genes. Our findings reveal how
24 SCF^{Met30} dynamically senses redox cues to regulate synthesis of these special amino acids, and
25 further highlight the mechanistic diversity in E3 ligase-substrate relationships.

26 27 INTRODUCTION

28
29 The biosynthesis of sulfur-containing amino acids supplies cells with increased levels of cysteine
30 and methionine, as well as their downstream metabolites glutathione and S-adenosylmethionine
31 (SAM). Glutathione serves as a redox buffer to maintain the reducing environment of the cell and
32 provide protection against oxidative stress, while SAM serves as the methyl donor for nearly all
33 methyltransferase enzymes (Ljungdahl and Daignan-Fornier, 2012, Cantoni, 1975). In the yeast
34 *Saccharomyces cerevisiae*, biosynthesis of all sulfur metabolites can be performed *de novo* via
35 enzymes encoded in the gene transcriptional network known as the *MET* regulon. Activation of
36 the *MET* gene transcriptional program under conditions of sulfur starvation relies on the
37 transcription factor Met4 and additional transcriptional co-activators that allow Met4 to be
38 recruited to the *MET* genes (Kuras et al., 1996, Blaiseau and Thomas, 1998).

39
40 When yeast cells sense sufficiently high levels of sulfur in the environment, the *MET* gene
41 transcriptional program is negatively regulated by the activity of the SCF E3 ligase Met30
42 (SCF^{Met30}) through ubiquitination of the master transcription factor Met4 (Kaiser et al., 2000).
43 Met4 is unique as an E3 ligase substrate as it contains an internal ubiquitin interacting motif (UIM)
44 which folds in and caps the growing ubiquitin chain generated by SCF^{Met30}, resulting in a
45 proteolytically stable but transcriptionally inactive oligo-ubiquitinated state (Flick et al., 2006).
46 Upon sulfur starvation, SCF^{Met30} ceases to ubiquitinate Met4, allowing Met4 to become
47 deubiquitinated and transcriptionally active.

48
49 Since its discovery, much effort has gone into understanding how Met30 senses the sulfur status
50 of the cell. Several mechanisms have been attributed to Met30 to describe how Met4 and itself
51 work together to regulate levels of *MET* gene transcripts in response to the availability of sulfur or
52 the presence of toxic heavy metals (Thomas et al., 1995). After the discovery that Met30 is an E3

53 ligase that negatively regulates Met4 through ubiquitin-dependent and both proteolysis-dependent
54 and independent mechanisms (Rouillon et al., 2000, Flick et al., 2004, Kuras et al., 2002), it was
55 found that Met30 dissociates from SCF complexes upon cadmium addition, resulting in the
56 disruption of the aforementioned ubiquitin-dependent regulatory mechanisms (Barbey et al.,
57 2005). It was later reported that this cadmium-specific dissociation of Met30 from SCF complexes
58 is mediated by the Cdc48/p97 AAA+ ATPase complex, and that Met30 ubiquitination is required
59 for Cdc48 to strip Met30 from these complexes (Yen et al., 2012). In parallel, attempts to identify
60 the sulfur metabolic cue sensed by Met30 suggested that cysteine, or possibly some downstream
61 metabolite, was required for the degradation of Met4 by SCF^{Met30}, although glutathione was
62 reportedly not involved in this mechanism (Hansen and Johannesen, 2000, Menant et al., 2006).
63 A genetic screen for mutants that fail to repress *MET* gene expression found that *cho2Δ* cells,
64 which are defective in the synthesis of phosphatidylcholine (PC) from phosphatidylethanolamine
65 (PE), results in elevated SAM levels and deficiency in cysteine levels (Sadhu et al., 2014).
66 However, while Met30 and Met4 have been studied extensively for over two decades, the
67 biochemical mechanisms by which Met30 senses and responds to the presence or absence of sulfur
68 remains incomplete (Sadhu et al., 2014).

69

70 Herein, we utilize prototrophic yeast strains grown in sulfur-rich and sulfur-free respiratory
71 conditions to elucidate the mechanism by which Met30 senses sulfur. Using a combination of *in*
72 *vivo* and *in vitro* experiments, we find that instead of sensing any single sulfur-containing
73 metabolite, Met30 indirectly senses the levels of sulfur metabolites in the cell by acting as a sensor
74 of redox state. We describe a novel mechanism by which an F-box protein can be regulated through
75 the use of multiple cysteine residues as redox sensors that, upon oxidation, disrupt binding of the
76 E3 ligase to its target to enable the activation of a coordinated transcriptional response.

77

78 RESULTS

79

80 SYNTHESIS OF CYSTEINE IS MORE IMPORTANT THAN METHIONINE FOR MET4 81 UBIQUITINATION

82

83 Previous work in our lab has characterized the metabolic and cellular response of yeast cells
84 following switch from rich lactate media (YPL) to minimal lactate media (SL) (Wu and Tu, 2011,
85 Sutter et al., 2013, Laxman et al., 2013, Kato et al., 2019, Yang et al., 2019, Ye et al., 2017, Ye et
86 al., 2019). Under such respiratory conditions, yeast cells engage regulatory mechanisms that might
87 otherwise be subject to glucose repression. Among other phenotypes, this switch results in the
88 acute depletion of sulfur metabolites and the activation of the *MET* gene regulon (Sutter et al.,
89 2013, Ye et al., 2019). To better study the response of yeast cells to sulfur starvation, we
90 reformulated our minimal lactate media to contain no sulfate, as prototrophic yeast can assimilate
91 sulfur in the form of inorganic sulfate into reduced sulfur metabolites. After switching cells from
92 YP lactate media (Rich) to the new minimal sulfur-free lactate media (-Sulfur), we found that

93 Met30 and Met4 quickly respond to sulfur starvation through the extensively studied ubiquitin-
94 dependent mechanisms regulating Met4 activity (Figure 1A) (Yen et al., 2005, Flick et al., 2006,
95 Barbey et al., 2005, Kaiser et al., 2000, Flick et al., 2004). As previously observed, the
96 deubiquitination of Met4 resulted in the activation of the *MET* genes (Figure 1B) and corresponded
97 well with changes in observed sulfur metabolite levels (Figure 1C). Addition of sulfur metabolites
98 quickly rescued Met30 activity and resulted in the re-ubiquitination of Met4 and the repression of
99 the *MET* genes.

100

101 As previously noted, Met4 activation in response to sulfur starvation results in the emergence of a
102 second, faster-migrating proteoform of Met30, which disappears after rescuing yeast cells with
103 sulfur metabolites (Sadhu et al., 2014). We found that the appearance of this proteoform is
104 dependent on both *MET4* and new translation, as it was not observed in either *met4Δ* cells or cells
105 treated with cycloheximide during sulfur starvation (Figure S1A and C). Additionally, this
106 proteoform persists after rescue with a sulfur source in the presence of a proteasome inhibitor
107 (Figure S1B).

108

109 We hypothesized that this faster-migrating proteoform of Met30 might be the result of translation
110 initiation at an internal methionine residue. In support of this possibility, mutation of methionine
111 residues 30, 35, and 36 to alanine blocked the appearance of a lower form during sulfur starvation
112 (Figure S1D). Conversely, deletion of the first 20 amino acids containing the first three methionine
113 residues of Met30 resulted in expression of a Met30 proteoform that migrated at the apparent
114 molecular weight of the wild type short form and did not generate a new, even-faster migrating
115 proteoform under sulfur starvation (Figure S1D). Moreover, the Met30^{M30/35/36A} and Met30^{Δ1-20}
116 strains expressing either solely the long or short form of the Met30 protein had no obvious
117 phenotype with respect to Met4 ubiquitination or growth in high or low sulfur media (Figure S1E).
118 We conclude that the faster-migrating proteoform of Met30 that is produced during sulfur
119 starvation has no discernible effect on sulfur metabolic regulation under these conditions.

120

121 The sulfur amino acid biosynthetic pathway is bifurcated into two branches at the central
122 metabolite homocysteine, where this precursor metabolite commits either to the production of
123 cysteine or methionine (Figure 1E). After confirming Met30 and Met4 were responding to sulfur
124 starvation as expected, we sought to determine whether the cysteine or methionine branch of the
125 sulfur metabolic pathway was sufficient to rescue Met30 E3 ligase activity and re-ubiquitinate
126 Met4 after sulfur starvation. To determine whether the synthesis of methionine is necessary to
127 rescue Met30 activity, cells lacking methionine synthase (*met6Δ*) were fed either homocysteine or
128 methionine after switching to sulfur-free lactate (-Sulfur) media. Interestingly, cells fed
129 homocysteine were still able to ubiquitinate and degrade Met4, while methionine-fed cells
130 appeared to oligo-ubiquitinate and stabilize Met4 (Figure 1D). These observations are consistent
131 with previous reports and suggest Met30 and Met4 interpret sulfur sufficiency through both
132 branches of sulfur metabolism to a degree (Hansen and Johannesen, 2000, Kaiser et al., 2000,

133 Kuras et al., 2002, Flick et al., 2004, Menant et al., 2006, Sadhu et al., 2014), with the stability of
134 Met4, but not the E3 ligase activity of Met30, apparently dependent on the methionine branch.

135

136 To determine whether Met30 specifically responds to cysteine, cells lacking cystathionine beta-
137 lyase (*str3Δ*), the enzyme responsible for the conversion of cystathionine to homocysteine, were
138 starved of sulfur and fed either cysteine or methionine. This mutant is incapable of synthesizing
139 methionine from cysteine via the two-step conversion of cysteine into the common precursor
140 metabolite homocysteine. Our results show cysteine was able to rescue Met30 activity even in a
141 *str3Δ* mutant, further suggesting cysteine or a downstream metabolite, and not methionine, as the
142 signal of sulfur sufficiency for Met30 (Figure 1D).

143

144 **CYSTEINE RESIDUES IN MET30 ARE OXIDIZED DURING SULFUR STARVATION**

145

146 The synthesis of cysteine from homocysteine contributes to the production of the downstream
147 tripeptide metabolite glutathione (GSH), which exists at millimolar concentrations in cells and is
148 the major cellular reductant for buffering against oxidative stress (Cuozzo and Kaiser, 1999, Wu
149 et al., 2004). Specifically, glutathione serves to neutralize reactive oxygen species such as
150 peroxides and free radicals, detoxify heavy metals, and preserve the reduced state of protein thiols
151 (Pompella et al., 2003, Penninckx, 2000). Considering the relatively high number of cysteine
152 residues in Met30 (Figure 2A), we sought to determine if these residues might become oxidized
153 during acute sulfur starvation. Utilizing the thiol-modifying agent methoxy-PEG-maleimide
154 (mPEG2K-mal), which adds ~2 kDa per reduced cysteine residue, we assessed Met30 cysteine
155 oxidation *in vivo* by Western blot. Theoretically, full modification of the 23 cysteines in Met30 by
156 mPEG2K-mal should significantly shift the apparent molecular weight of Met30 by ~45-50 kDa.
157 As expected, Met30 in sulfur-replete rich media migrates at ~140 kDa (Figure 2B, first lane),
158 nicely corresponding to the modification of most if not all of its 23 cysteine residues, suggesting
159 they are all in the reduced state while sulfur levels are high and Met4 is being negatively regulated.
160 However, after shifting into sulfur-free minimal lactate media, Met30 migrates at ~80 kDa —
161 suggesting the majority of its cysteine residues are rapidly becoming oxidized *in vivo* following
162 acute sulfur starvation (Figure 2B, second and third lane). In contrast, the loading control Rpn10
163 contains a single cysteine residue, and did not exhibit significant oxidation within the same time
164 period of sulfur starvation. As expected, repletion of sulfur metabolites led to the reduction and
165 modification of Met30's cysteine residues by mPEG2K-mal to the extent seen in the rich media
166 condition. Such oxidation and re-reduction of Met30 cysteines corresponds well with Met4
167 ubiquitination status (Figure 2B). Additionally, when cells were grown in sulfur-free media
168 containing glucose (SFD) as the carbon source, Met30 also becomes oxidized, although on a
169 slower timescale — suggesting this mechanism is not specific to yeast grown under non-
170 fermentable conditions (Figure 2C).

171

172 Considering the link between sulfur starvation and oxidative stress, we next assessed whether
173 simply changing the redox state of sulfur-starved cells could mimic sulfur repletion with respect
174 to Met30 E3 ligase activity. Addition of the potent, membrane-permeable reducing agent DTT to
175 yeast cells starved of sulfur readily reversed Met30 cysteine oxidation. DTT also resulted in the
176 partial re-ubiquitination of Met4, suggesting that Met30 cysteine redox status influences its
177 ubiquitination activity against Met4 (Figure 2D). Taken together, these data strongly suggest
178 cysteine residues within Met30 are poised to become rapidly oxidized in response to sulfur
179 starvation, which is correlated with the deubiquitination of its substrate Met4.

180

181 **MET30 CYSTEINE POINT MUTANTS EXHIBIT DYSREGULATED SULFUR SENSING** 182 ***IN VIVO***

183

184 After establishing Met30 cysteine redox status as an important factor in sensing sulfur starvation,
185 we sought to determine whether specific residues played key roles in the sensing mechanism.
186 Through site-directed mutagenesis of Met30 cysteines individually and in clusters (Figure S2A
187 and B), we observed that mutation of cysteines in the WD-40 repeat regions of Met30 with the
188 highest concentration of cysteine residues (WD-40 repeat regions 4 and 8) resulted in dysregulated
189 Met4 ubiquitination status (Figure 3A) and *MET* gene expression (Figure 3B). Specifically,
190 conservatively mutating these cysteines to serine residues mimics the reduced state of the Met30
191 protein, resulting in constitutive ubiquitination of Met4 by Met30 even when cells are starved of
192 sulfur. The mixed population of ubiquitinated and deubiquitinated Met4 in the mutant strains
193 resulted in reduced induction of *SAM1* and *GSH1*, while *MET17* appears to be upregulated in the
194 mutants but is largely insensitive to the changes in the sulfur status of the cell. Interestingly, a
195 single cysteine to serine mutant, C414S, phenocopies the grouped cysteine to serine mutants
196 C414/426/436/439S (data not shown) and C614/616/622/630S. These mutants also exhibit slight
197 growth phenotypes when cultured in both rich and –sulfur lactate media supplemented with
198 homocysteine (Figure 3C). Furthermore, these point mutants only effect Met4 ubiquitination in
199 the context of sulfur starvation, as strains expressing these mutants exhibited a normal response to
200 cadmium as evidenced by rapid deubiquitination of Met4 (Figure S2C).

201

202 **MET30 CYSTEINE OXIDATION DISRUPTS UBIQUITINATION AND BINDING OF** 203 ***MET4 IN VITRO***

204

205 Having observed that Met30 cysteine redox status is correlated with Met4 ubiquitination status *in*
206 *vivo*, we next sought to determine whether the sulfur/redox-sensing ability of SCF^{Met30} E3 ligase
207 activity could be reconstituted *in vitro*. To this end, we performed large scale immuno-purifications
208 of SCF^{Met30-Flag} to pull down Met30 and its interacting partners in both high and low sulfur
209 conditions for *in vitro* ubiquitination assays with recombinantly purified E1, E2, and Met4 (Figure
210 4A). Initial *in vitro* ubiquitination experiments showed little difference in activity between the two

211 conditions, mirroring prior efforts to demonstrate differential activity of the Met30 E3 ligase in
212 response to stimuli that effect its activity *in vivo* (Figure S3A) (Barbey et al., 2005).

213

214 Since the cysteine residues within Met30 became rapidly oxidized in sulfur-free conditions, the
215 addition of DTT as a standard component in our IP buffer and in *in vitro* ubiquitination reactions
216 could potentially reduce oxidized Met30 cysteines and alter its ubiquitination activity towards
217 Met4. To test this possibility, we next performed the Met30 IP and *in vitro* assay in the complete
218 absence of reducing agent. Strikingly, we observed little to no ubiquitination activity in these
219 conditions (Fig. S3B), suggesting that oxidized Met30 exhibits significantly reduced
220 ubiquitination activity.

221

222 To more rigorously test the effect of reducing agents on the activity of immunopurified SCF^{Met30},
223 we performed in parallel the Met30-Flag IP with cells grown in both high and low sulfur
224 conditions, with and without reducing agent in the IP. Silver stains of the eluted co-IP Met30
225 complexes showed similar levels of total protein overall and little difference in the abundance of
226 major binding partners between the four conditions (Figure S3C). Western blots of the co-IP
227 samples for the Cdc53/cullin scaffold showed similar binding between the samples with the
228 exception of the –sulfur, –DTT sample which had approximately a third of the amount of Cdc53
229 bound to Met30 (Figure S3D). We suspect this difference is due to the canonical regulation of SCF
230 E3 ligases, which uses cyclic changes in the affinity of Skp1/F-box protein heterodimers to the
231 cullin scaffold based on binding between the F-box protein and its substrate (Reitsma et al., 2017).
232 After performing the initial IP and washing the beads in buffer with and without reducing agent,
233 the final wash step and Flag peptide elution were done without reducing agent in the buffer for all
234 four IP conditions in order to remove any residual reducing agent from the final ubiquitination
235 reaction, which was also performed without reducing agent. A small aliquot of the rich and –sulfur
236 “–DTT” immunopurified SCF^{Met30} was transferred to a new tube and treated with 5 mM TCEP, a
237 non-thiol, phosphine-based reducing agent, for approximately 30 min while the *in vitro*
238 ubiquitination assays were set up to test if the low activity of the oxidized SCF^{Met30} complex could
239 be rescued by treating with another reducing agent before addition to the final reaction. The data
240 clearly demonstrate that the presence of reducing agent in the IP and wash buffer, but not in the
241 elution or final reaction, significantly increased the E3 ligase activity of SCF^{Met30} *in vitro* regardless
242 of whether the cells were grown in high (Figure 4C) or low sulfur media (Figure 4D). Further
243 supporting our hypothesis, brief treatment of the oxidized –DTT IP complex with TCEP
244 (–DTT/+TCEP) rescued the activity of the E3 complex *in vitro* (Figures 4B and C). The same +/-
245 – DTT *in vitro* ubiquitination experiment done with the C414S and C614/616/622/630S Met30
246 mutants showed lower E3 ligase activity overall relative to wild type Met30, but smaller
247 differences between the plus and minus reducing agent condition (Figure S4A).

248

249 As SCF^{Met30} E3 ligase activity *in vitro* is independent of the sulfur-replete or -starved state of the
250 cells from which the co-IP concentrate is produced, and that the activity of the SCF^{Met30} co-IP

251 concentrate purified in the absence of reducing agent can be rescued by treatment with another
252 reducing agent, we hypothesized that the low E3 ligase activity of SCF^{Met30} purified in the absence
253 of reducing agent is due to decreased binding between Met30 and Met4, and not decreased binding
254 between Met30 and the other core SCF components. To test this possibility, lysate for “rich” and
255 “–sulfur” cells was prepared and each was split into three groups, with either reducing agent
256 (+DTT), the thiol-specific oxidizing agent tetramethylazodicarboxamide (+Diamide), or control
257 (–DTT) (Figure 4A). Met30-Flag IPs were performed as previously described for the *in vitro*
258 ubiquitination assay, except instead of eluting Met30 off of the beads, the +DTT, –DTT, and
259 +Diamide beads were each split into two tubes containing IP buffer ±DTT and bacterially purified
260 Met4. The beads were incubated with purified Met4 prior to washing with IP buffer with or without
261 DTT. We observed a clear, DTT-dependent increase in the fraction of Met4 bound to the Met30-
262 Flag beads, with the “+DTT” Met30 IP showing a larger initial amount of bound Met4 compared
263 to the “–DTT” Met30 IP, with even less Met4 bound to the “+Diamide” Met30-Flag beads.
264 Consistent with our hypothesis, the addition of DTT to the Met4 co-IP with “–DTT” or
265 “+Diamide” Met30-Flag beads restored the Met30/Met4 interaction to the degree seen in the
266 “+DTT” Met30-Flag beads. We then performed the same experiment with our Met30 cysteine
267 point mutants. The amount of Met4 bound to these mutants was less sensitive to the presence or
268 absence of reducing agent (Figure S4B). Collectively, these data suggest that the reduced form of
269 key cysteine residues in Met30 enables it to engage its Met4 substrate and facilitate ubiquitination.

270

271 DISCUSSION

272

273 The unique redox chemistry offered by sulfur and sulfur-containing metabolites renders many of
274 the biochemical reactions required for life possible. The ability to carefully regulate the levels of
275 these sulfur-containing metabolites is of critical importance to cells as evidenced by an exquisite
276 sulfur-sparing response. Sulfur starvation induces the transcription of *MET* genes and specific
277 isozymes, which themselves contain few methionine and cysteine residues (Fauchon et al., 2002).
278 Furthermore, along with the dedicated cell cycle F-box protein Cdc4, Met30 is the only other
279 essential F-box protein in yeast, linking sulfur metabolite levels to cell cycle progression (Su et
280 al., 2005, Su et al., 2008). Our findings highlight the intimate relationship between sulfur
281 metabolism and redox chemistry in cellular biology, revealing that the key sensor of sulfur
282 metabolite levels in yeast, Met30, is regulated by reversible cysteine oxidation. Such oxidation of
283 Met30 cysteines in turn influences the ubiquitination status and transcriptional activity of the
284 master sulfur metabolism transcription factor Met4. While much work has been done to
285 characterize the molecular basis of sulfur metabolic regulation in yeast between Met30 and Met4,
286 this work describes the biochemical basis for sulfur sensing by the Met30 E3 ligase (Figure 5).

287

288 The ability of Met30 to act as a cysteine redox-responsive E3 ligase is unique in *Saccharomyces*
289 *cerevisiae*, but is reminiscent of the redox-responsive Keap1 E3 ligase in humans. In humans,
290 Keap1 ubiquitinates and degrades its Nrf2 substrate to regulate the cellular response to oxidative

291 stress. When cells are exposed to electrophilic metabolites or oxidative stress, key cysteine
292 residues are either alkylated or oxidized into disulfides, resulting in conformational changes that,
293 in turn, either disrupt Keap1 association with Cul3 or Nrf2, both leading to Nrf2 activation
294 (Yamamoto et al., 2018). Our data suggest that in response to sulfur starvation, Met30 can still
295 maintain its association with the SCF E3 ligase cullin scaffold, but that treatment of the oxidized
296 complex with reducing agent is sufficient to stimulate ubiquitination of Met4 *in vitro*. This, along
297 with the *in vivo* and *in vitro* Met30 cysteine point mutant data, leads us to conclude that it is the
298 ability of Met30 to bind its substrate Met4 that is being disrupted by cysteine oxidation.

299

300 Previous work on the yeast response to cadmium toxicity demonstrated that Met30 is stripped from
301 SCF complexes by the p97/Cdc48 segregase upon treatment with cadmium, suggesting that like
302 Keap1, Met30 can utilize both dissociation from SCF complexes and disrupted interaction with
303 Met4 to modulate Met4 transcriptional activation (Barbey et al., 2005, Yen et al., 2012). Recent
304 work on the sensing of oxidative stress by Keap1 has found that multiple cysteines in Keap1 can
305 act cooperatively to form disulfides, and that the use of multiples cysteines to form different
306 disulfide bridges creates an “elaborate fail-safe mechanism” to sense oxidative stress (Suzuki et
307 al., 2019). In light of our findings, we suspect Met30 might similarly use multiple cysteine residues
308 in a cooperative disulfide formation mechanism to disrupt the binding interface between Met30
309 and Met4, but more work will be needed to demonstrate this definitively. It is worth noting the
310 curious spacing and clustering of cysteine residues in Met30, with the highest density and closest
311 spacing of cysteines found in two WD-40 repeats that are expected to be directly across from each
312 other in the 3D structure (Figure 2A). That the mutation of these cysteine clusters to serine have
313 the largest *in vivo* effect, but mutation of any one cysteine to serine (with the notable exception of
314 Cys414) has no effect, implies some built-in redundancy in the cysteine-based redox-sensing
315 mechanism (Figure S2B). We speculate that the oxidation of the cysteines in the WD-40 repeat
316 region of Met30 work cooperatively to produce structural changes that position Cys414 to make a
317 key disulfide linkage that disrupts the interaction with Met4.

318

319 It was previously hypothesized that an observed, faster-migrating proteoform of Met30 might be
320 involved in the regulation of sulfur metabolism (Sadhu et al., 2014). We deduced that the lower
321 form of Met30 does appear to be the result of transcriptionally-guided, alternative translational
322 initiation. However, this faster-migrating proteoform appears dispensable for sulfur metabolic
323 regulation under the conditions we examined. It is curious that such an ostensibly obvious feedback
324 loop between Met30 and Met4 would appear to have little to no effect on sulfur metabolic
325 regulation. However, during sulfur starvation, a decrease in global translation coincides with an
326 increase in ribosomes containing one, instead of two, methyl groups at universally conserved,
327 tandem adenosines near the 3’end of 18S rRNA (Liu et al.) We speculate that these ribosomes
328 might preferentially translate *MET* gene mRNAs, as well as preferentially initiate translation at the
329 internal 30, 35, and 36th methionine residues of Met30.

330

331 The utilization of a redox mechanism for Met30 draws interesting comparisons to the regulation
332 of Met4 via ubiquitination in that both mechanisms are rapid and readily reversible, require no
333 new RNA or protein synthesis, and there is no requirement for the consumption of sulfur
334 equivalents so as to spare them for use in *MET* gene translation under conditions of sulfur scarcity.
335 It is also striking that while Met30 contains many cysteine residues, Met4 contains none – which
336 has the consequence that as Met30 cysteines are oxidized, there is no possibility that Met4 can
337 make an intermolecular disulfide linkage that might interfere with its release and recruitment to
338 the promoters of *MET* genes. Upon repletion of sulfur metabolites, cellular reducing capacity is
339 restored, and Met30 cysteine reduction couples the regulation of *MET* gene activation to sulfur
340 assimilation, both of which require significant reducing equivalents.

341
342 Lastly, we highlight the observation that nearly all of the Met30 protein becomes rapidly oxidized
343 within 15 min of sulfur starvation, in contrast to other nucleocytosolic proteins (Fig. 2B). Bulk
344 levels of oxidized versus reduced glutathione are also minimally changed within this timeframe.
345 These considerations suggest that Met30 is either located in a redox-responsive microenvironment
346 within cells, or that key cysteine residues such as Cys414 are predisposed to becoming oxidized
347 to subsequently inhibit binding and ubiquitination of Met4. Future structural characterization of
348 SCF^{Met30} in its reduced and oxidized states may reveal the underlying basis of its exquisite
349 sensitivity to, and regulation by, oxidation. Nonetheless, along with SoxR and OxyR transcription
350 factors in *E. coli* (Imlay, 2013) the Yap1 transcription factor in yeast (Herrero et al., 2008), and
351 Keap1 in mammalian cells, our studies add the F-box protein Met30 to the exclusive list of bona
352 fide cellular redox sensors that can initiate a transcriptional response.

353 354 **ACKNOWLEDGMENTS**

355
356 We thank members of the Tu lab, Deepak Nijhawan, Hongtao Yu, and George DeMartino for
357 helpful discussions. This work was supported by NIH R01GM094314, R35GM136370, and an
358 HHMI-Simons Faculty Scholars Award to B.P.T.

359 360 **AUTHOR CONTRIBUTIONS**

361
362 This study was conceived by Z.J. and B.P.T. B.M.S. performed Met30 cysteine point mutant strain
363 construction, Y.W. performed cysteine point mutant cloning and Cdc34 protein purification, and
364 all remaining experiments were directed and performed by Z.J. The paper was written by Z.J. and
365 B.P.T. and has been approved by all authors.

366 367 **DECLARATION OF INTERESTS**

368
369 The authors declare no competing interests.

370

371 **EXPERIMENTAL PROCEDURES**

372

373 **Yeast strains, construction, and growth media**

374 The prototrophic CEN.PK strain background (van Dijken et al., 2000) was used in all experiments.
375 Strains used in this study are listed in Table S1. Gene deletions were carried out using either tetrad
376 dissection or standard PCR-based strategies to amplify resistance cassettes with appropriate
377 flanking sequences, and replacing the target gene by homologous recombination (Longtine et al.,
378 1998). C-terminal epitope tagged strains were similarly made with the PCR-based method to
379 amplify resistance cassettes with flanking sequences. Point mutations were made by cloning the
380 gene into the tagging plasmids, making the specific point mutation(s) by PCR, and amplifying and
381 transforming the entire gene locus and resistance markers with appropriate flanking sequences
382 using the lithium acetate method.

383

384 Media used in this study: YPL (1% yeast extract, 2% peptone and 2% lactate); sulfur-free glucose
385 and lactate media (SFD/L) media composition is detailed in Table S2, with glucose or lactate
386 diluted to 2% each; YPD (1% yeast extract, 2% peptone and 2% glucose).

387

388 **Whole cell lysate Western blot preparation**

389 Five OD₆₀₀ units of yeast culture were quenched in 15% TCA for 15 min, pelleted, washed with
390 100% EtOH, and stored at -20°C. Cell pellets were resuspended in 325 µL EtOH containing 1
391 mM PMSF and lysed by bead beating. The lysate was separated from beads by inverting the
392 screwcap tubes, puncturing the bottom with a 23G needle, and spinning the lysate at 2,500xg into
393 an Eppendorf for 1 min. Beads were washed with 200 µL of EtOH and spun again before
394 discarding the bead-containing screwcap tube and pelleting protein extract at 21,000xg for 10 min
395 in the new Eppendorf tube. The EtOH was aspirated and EtOH precipitated protein pellets were
396 resuspended in 150 µL of sample buffer (200 mM Tris pH 6.8, 4% SDS, 20% glycerol, 0.2 mg/ml
397 bromophenol blue), heated at 42°C for 45 min, and debris was pelleted at 16,000xg for 3 min. DTT
398 was added to a final concentration of 25 mM and incubated at RT for 30 min before equivalent
399 amounts of protein were loaded onto NuPAGE 4-12% bis-tris or 3-8% tris-acetate gels. For protein
400 samples modified with mPEG2K-mal, an aliquot of the sample buffer resuspended protein pellets
401 was moved to a fresh Eppendorf and sample buffer containing 15 mM mPEG2K-mal was added
402 for a final concentration of 5 mM mPEG2K-mal before heating at 42°C for 45 min, pelleting
403 debris, and adding DTT.

404

405 **Western blots**

406 Western blots were carried out by transferring whole cell lysate extracts or *in vitro* ubiquitination
407 or binding assay samples onto 0.45 micron nitrocellulose membranes and wet transfers were
408 carried out at 300 mA constant for 90 min at 4°C. Membranes were incubated with ponceau S,
409 washed with TBST, blocked with 5% milk in TBST for 1 h, and incubated with 1:5000 Mouse
410 anti-FLAG M2 antibody (Sigma, Cat#F3165), 1:5000 Mouse anti-HA(12CA5) (Roche,

411 Ref#11583816001), 1:50,000 Rabbit anti-RPN10 (Abcam, ab98843), or 1:3000 Goat anti-Cdc53
412 (Santa Cruz, yC-17) in 5% milk in TBST overnight at 4°C. After discarding primary antibody,
413 membranes were washed 3 times for 5 min each before incubation with appropriate HRP-
414 conjugated secondary antibody for 1 h in 5% milk/TBST. Membranes were then washed 3 times
415 for 5 min each before incubating with Pierce ECL western blotting substrate and exposing to film.
416

417 **RNA Extraction and Real Time Quantitative PCR (RT-qPCR) Analysis**

418 RNA isolation of five OD₆₀₀ units of cells under different growth conditions was carried out
419 following the manufacture manual using MasterPure yeast RNA purification kit (epicentre). RNA
420 concentration was determined by absorption spectrometer. 5 µg RNA was reverse transcribed to
421 cDNA using Superscript III Reverse Transcriptase from Invitrogen. cDNA was diluted 1:100 and
422 real-time PCR was performed in triplicate with iQ SYBR Green Supermix from BioRad.
423 Transcripts levels of genes were normalized to ACT1. All the primers used in RT-qPCR have
424 efficiency close to 100%, and their sequences are listed below.
425

426 ACT1_RT_F TCCGGTGATGGTGTTACTCA
427 ACT1_RT_R GGCCAAATCGATTCTCAAAA
428 MET17_RT_F CGGTTTCGGTGGTGTCTTAT
429 MET17_RT_R CAACAACCTGAGCACCAGAAAG
430 GSH1_RT_F CACCGATGTGGAAACTGAAGA
431 GSH1_RT_R GGCATAGGATTGGCGTAACA
432 SAM1_RT_F CAGAGGGTTTGCCTTTGACTA
433 SAM1_RT_R CTGGTCTCAACCACGCTAAA
434

435 **Metabolite extraction and quantitation**

436 Intracellular metabolites were extracted from yeast using a previous established method (Tu et al.,
437 2007). Briefly, at each time point, ~12.5 OD₆₀₀ units of cells were rapidly quenched to stop
438 metabolism by addition into 37.5 mL quenching buffer containing 60% methanol and 10 mM
439 Tricine, pH 7.4. After holding at -40°C for at least 3 min, cells were spun at 5,000xg for 2 min at
440 0°C, washed with 1 mL of the same buffer, and then resuspended in 1 mL extraction buffer
441 containing 75% ethanol and 0.1% formic acid. Intracellular metabolites were extracted by
442 incubating at 75°C for 3 min, followed by incubation at 4°C for 5 min. Samples were spun at
443 20,000xg for 1 min to pellet cell debris, and 0.9 mL of the supernatant was transferred to a new
444 tube. After a second spin at 20,000xg for 10 min, 0.8 mL of the supernatant was transferred to a
445 new tube. Metabolites in the extraction buffer were dried using SpeedVac and stored at -80°C
446 until analysis. Methionine, SAM, SAH, cysteine, GSH and other cellular metabolites were
447 quantitated by LC-MS/MS with a triple quadrupole mass spectrometer (3200 QTRAP, AB SCIEX)
448 using previously established methods (Tu et al., 2007). Briefly, metabolites were separated
449 chromatographically on a C18-based column with polar embedded groups (Synergi Fusion-RP,
450 150 3 2.00 mm 4 micron, Phenomenex), using a Shimadzu Prominence LC20/SIL-20AC HPLC-
451 autosampler coupled to the mass spectrometer. Flow rate was 0.5 ml/min using the following

452 method: Buffer A: 99.9% H₂O/0.1% formic acid, Buffer B: 99.9% methanol /0.1% formic acid. T
453 = 0 min, 0% B; T = 4 min, 0% B; T = 11 min, 50% B; T = 13 min, 100% B; T = 15 min, 100% B,
454 T = 16 min, 0% B; T = 20 min, stop. For each metabolite, a 1 mM standard solution was infused
455 into a Applied Biosystems 3200 QTRAP triple quadrupole-linear ion trap mass spectrometer for
456 quantitative optimization detection of daughter ions upon collision-induced fragmentation of the
457 parent ion [multiple reaction monitoring (MRM)]. The parent ion mass was scanned for first in
458 positive mode (usually MW + 1). For each metabolite, the optimized parameters for quantitation
459 of the two most abundant daughter ions (i.e., two MRMs per metabolite) were selected for
460 inclusion in further method development. For running samples, dried extracts (typically 12.5 OD
461 units) were resuspended in 150 mL 0.1% formic acid, spun at 21,000xg for 5 min at 4°C, and 125
462 µL was moved to a fresh Eppendorf. The 125 µL was spun again at 21,000xg for 5 min at 4°C,
463 and 100 µL was moved to mass-spec vials for injection (typically 50 µL injection volume). The
464 retention time for each MRM peak was compared to an appropriate standard. The area under each
465 peak was then quantitated by using Analyst® 1.6.3, and were re-inspected for accuracy.
466 Normalization was done by normalizing total spectral counts of a given metabolite by OD₆₀₀ units
467 of the sample. Data represents the average of two biological replicates.

468

469 **Protein purification**

470 6xHis-Uba1 (E1) was purified as previously described (Petroski and Deshaies, 2005), with the
471 exception that the strain was made in the cen.pk background and the His₆-tag was appended to the
472 N-terminus of Uba1. Additionally, lysis was performed by cryomilling frozen yeast pellets by
473 adding the pellet to a pre-cooled 50 ml milling jar containing a 20 mm stainless steel ball. Yeast
474 cell lysis was performed by milling in 3 cycles at 25 Hz for 3 min and chilling in liquid nitrogen
475 for 1 min. Lysate was made by adding 4 ml of buffer for every gram of cryomilled yeast powder,
476 and clarification was performed at 35,000xg instead of 50,000xg.

477

478 Cdc34-6xHis (E2) similarly was purified according to previously described protocols (Petroski
479 and Deshaies, 2005), with the following exceptions; the CDC34 ORF was cloned into pHis
480 parallel vector such that the N-terminal His tag was eliminated from the vector while incorporating
481 a C-terminal 6xHis tag by PCR. BL21 transformants were grown in LB medium and expression
482 was induced by addition of 0.1 mM IPTG. Cells were lysed by sonication and clarification was
483 done by spinning at 35,000xg for 20 min at 4°C before the Ni-NTA purification was performed as
484 previously described (Petroski and Deshaies, 2005).

485

486 His-SUMO-Met4-Strep-tagII-HA was purified by cloning the MET4 ORF into pET His6 Sumo
487 vector while incorporating a C-terminal Strep-tagII and a single HA tag by PCR. BL21
488 transformants were grown in 2 liters LB medium and induced by addition of 0.1 mM IPTG O/N
489 at 16°C at 200 rpm. Cell pellets were collected and lysed by sonication in buffer containing 50
490 mM Tris pH 7.5, 300 mM NaCl, 10% glycerol, 20 mM imidazole, 1 mM PMSF, 10 µM leupeptin,
491 50 mM NaF, 5 µM pepstatin, 0.5% NP-40, and 2x roche EDTA-free protease inhibitor cocktail

492 tablet. Lysate was clarified by centrifugation at 35,000xg for 20 min at 4°C and the supernatant
493 was transferred to a 50 ml conical and Met4 was batch purified with 1.5 ml of Ni-NTA agarose by
494 incubating for 30 min at 4°C. After spinning down the Ni-NTA agarose, the supernatant was
495 removed and the agarose was resuspended in the same buffer and moved to a gravity flow column
496 and washed 3 times with 50 mM Tris pH 7.5, 300 mM NaCl, 10% glycerol, and 20 mM imidazole
497 before elution with the same buffer containing 200 mM imidazole. Eluted Met4 was then run over
498 2 ml of Strep-Tactin Sepharose in a 10 ml gravity flow column, washed with 5 CVs Strep-Tactin
499 wash buffer (100 mM Tris pH 8.0, 150 mM NaCl), and eluted by diluting 1 ml 10X Strep-Tactin
500 Elution buffer in 9 ml Strep-Tactin wash buffer and collecting 1.5 ml fractions. Fractions
501 containing pure, full-length Met4 were pooled and concentrated while exchanging the buffer with
502 buffer containing 30 mM Tris pH 7.6, 100 mM NaCl, 5 mM MgCl₂, 15% glycerol, and 2 mM
503 DTT. Protein concentration was measured and 1 mg/ml aliquots were made and stored at -80°C.

504

505 SCF^{Met30-Flag} IP and *in vitro* ubiquitination assay

506 Strains containing Flag-tagged Met30 were grown in rich YPL media overnight to mid-late log
507 phase before dilution with more YPL and grown for 3 h before half of the culture was separated
508 and switched -sulfur SFL media for 15 min. Subsequently, approximately 3000 OD₆₀₀ units each
509 of YPL and SFL cultured yeast were spun down and frozen in liquid nitrogen. Frozen yeast pellets
510 were cryomilled by adding the pellet to a pre-cooled 50 ml milling jar containing a 20 mm stainless
511 steel ball. Yeast cell lysis was performed by milling in 3 cycles at 25 Hz for 3 min and chilling in
512 liquid nitrogen for 1 min. Cryomilled yeast powder (~ 4 grams) was moved to a 50 ml conical and
513 resuspended in 16 ml SCF IP buffer (50 mM Tris pH 7.5, 150 mM NaCl, 10 mM NaF, 1% NP-40,
514 1 mM EDTA, 5% glycerol) containing 10 μM leupeptin, 1 mM PMSF, 5 μM pepstatin, 100 μM
515 sodium orthovanadate, 2 mM 1, 10-phenanthroline, 1 μM MLN4924, 1X Roche EDTA-free
516 protease inhibitor cocktail tablet, and 1 mM DTT when specified. Small molecule inhibitors of
517 neddylation and deneddylation were included, and along with a short IP time, intended to minimize
518 exchange and preserve F-box protein/Skp1 substrate recognition modules (Reitsma et al., 2017).
519 The lysate was then briefly sonicated to shear DNA and subsequently clarified at 35,000xg for 20
520 min and the supernatant was incubated with with 50 μL of Thermo Fisher protein G dynabeads
521 (Cat# 10004D) DMP crosslinked to 25 μL of Mouse anti-FLAG M2 antibody (Sigma, Cat#F3165)
522 for 30 min at 4°C. The agarose was pelleted at 500xg for 5 min, the supernatant was aspirated, and
523 the magnetic beads transferred to an Eppendorf tube. The beads were washed 5 times with 1 ml
524 SCF IP buffer with or without DTT before elution with 1 mg/ml Flag peptide in PBS. The eluent
525 was concentrated in Amicon Ultra-0.5 centrifugal filter units with 10 kDa MW cutoffs to a final
526 volume of ~ 40 μL. Silver stains of the IPs were carried out using the Pierce Silver Stain for Mass
527 Spectrometry kit (Cat#24600) according to the manufacturers protocol. The *in vitro* ubiquitination
528 assay was performed by placing a PCR tube on ice and adding to it 29 μL of water, 8 μL of 5X
529 ubiquitination assay buffer (250 mM Tris pH 7.5, 5 mM ATP, 25 mM MgCl₂, 25% glycerol), 1.2
530 μL Uba1 (FC = 220 nM), 1.2 μL Cdc34 (FC = 880 nM), 0.5 μL yeast ubiquitin (Boston Biochem,
531 FC = 15.5 μM) and incubating at RT for 20 min. The PCR tubes were then placed back on ice and

532 20 μ L of water, 8 μ L of 5X ubiquitination assay buffer, 10 μ L of concentrated SCF^{Met30-Flag} IP,
533 and 2 μ L of purified Met4 (FC = 200 nM) were added, the tubes were moved back to RT, and 20
534 μ L aliquots of the reaction were removed, mixed with 2X sample buffer, and frozen in liquid
535 nitrogen over the time course.

536

537 **SCF^{Met30-Flag} IP and *in vitro* Met4 binding assay**

538 For the Met4 binding assay, yeast cell lysate was prepared as described for the ubiquitination
539 experiment, except that the lysate was split three ways, with 1 mM DTT, 1 mM
540 tetramethylazodicarboxamide (Diamide) (Sigma, Cat#D3648), or nothing added to the lysate prior
541 to centrifugation at 21,000xg for 30 min at 4°C. The supernatant was transferred to new tubes and
542 100 μ L of Thermo Fisher protein G dynabeads (Cat# 10004D) DMP crosslinked to 50 μ L of
543 Mouse anti-FLAG M2 antibody (Sigma, Cat#F3165) was divided evenly between the six Met30-
544 Flag IP conditions and incubated for 2 h at 4°C while rotating end over end. After incubation, the
545 beads were washed with IP buffer containing 1 mM DTT, 1 mM Diamide, or nothing twice before
546 a final wash with plain IP buffer. Each set of Met30-Flag bound beads prepared in the different IP
547 conditions was brought up to 80 μ L with plain IP buffer, and 40 μ L was dispensed to new tubes
548 containing 1 mL of IP buffer \pm 1 mM DTT and 1 μ g of purified recombinant Met4, and were
549 incubated for 2 h at 4°C while rotating end over end for a total of twelve Met4 co-IP conditions.
550 The beads were then collected, washed 3 times with IP buffer \pm 1 mM DTT, resuspended in 60 μ L
551 2X sample buffer, and heated at 70°C for 10 min before Western blotting for both Met4 and Met30.

552

553

554

555 **REFERENCES**

556

557 BARBEY, R., BAUDOUIN-CORNU, P., LEE, T. A., ROUILLON, A., ZARZOV, P., TYERS,
558 M. & THOMAS, D. 2005. Inducible dissociation of SCF(Met30) ubiquitin ligase
559 mediates a rapid transcriptional response to cadmium. *EMBO J*, 24, 521-32.

560 BLAISEAU, P. L. & THOMAS, D. 1998. Multiple transcriptional activation complexes tether
561 the yeast activator Met4 to DNA. *EMBO J*, 17, 6327-36.

562 CANTONI, G. L. 1975. Biological methylation: selected aspects. *Annu Rev Biochem*, 44, 435-
563 51.

564 CUOZZO, J. W. & KAISER, C. A. 1999. Competition between glutathione and protein thiols for
565 disulfide-bond formation. *Nature cell biology*, 1, 130-135.

566 FAUCHON, M., LAGNIEL, G., AUDE, J.-C., LOMBARDIA, L., SOULARUE, P., PETAT, C.,
567 MARGUERIE, G., SENTENAC, A., WERNER, M. & LABARRE, J. 2002. Sulfur
568 sparing in the yeast proteome in response to sulfur demand. *Molecular cell*, 9, 713-723.

569 FLICK, K., OUNI, I., WOHLSCHLEGEL, J. A., CAPATI, C., MCDONALD, W. H., YATES, J.
570 R. & KAISER, P. 2004. Proteolysis-independent regulation of the transcription factor
571 Met4 by a single Lys 48-linked ubiquitin chain. *Nat Cell Biol*, 6, 634-41.

572 FLICK, K., RAASI, S., ZHANG, H., YEN, J. L. & KAISER, P. 2006. A ubiquitin-interacting
573 motif protects polyubiquitinated Met4 from degradation by the 26S proteasome. *Nat Cell*
574 *Biol*, 8, 509-15.

575 HANSEN, J. & JOHANNESSEN, P. F. 2000. Cysteine is essential for transcriptional regulation
576 of the sulfur assimilation genes in *Saccharomyces cerevisiae*. *Molecular and General*
577 *Genetics MGG*, 263, 535-542.

578 HERRERO, E., ROS, J., BELLÍ, G. & CABISCOL, E. 2008. Redox control and oxidative stress
579 in yeast cells. *Biochimica et Biophysica Acta (BBA)-General Subjects*, 1780, 1217-1235.

580 IMLAY, J. A. 2013. The molecular mechanisms and physiological consequences of oxidative
581 stress: lessons from a model bacterium. *Nature Reviews Microbiology*, 11, 443-454.

582 KAISER, P., FLICK, K., WITTENBERG, C. & REED, S. I. 2000. Regulation of transcription by
583 ubiquitination without proteolysis: Cdc34/SCFMet30-mediated inactivation of the
584 transcription factor Met4. *Cell*, 102, 303-314.

585 KATO, M., YANG, Y. S., SUTTER, B. M., WANG, Y., MCKNIGHT, S. L. & TU, B. P. 2019.
586 Redox State Controls Phase Separation of the Yeast Ataxin-2 Protein via Reversible
587 Oxidation of Its Methionine-Rich Low-Complexity Domain. *Cell*, 177, 711-721 e8.

588 KURAS, L., CHEREST, H., SURDIN-KERJAN, Y. & THOMAS, D. 1996. A heteromeric
589 complex containing the centromere binding factor 1 and two basic leucine zipper factors,

- 590 Met4 and Met28, mediates the transcription activation of yeast sulfur metabolism. *EMBO*
591 *J*, 15, 2519-29.
- 592 KURAS, L., ROUILLON, A., LEE, T., BARBEY, R., TYERS, M. & THOMAS, D. 2002. Dual
593 regulation of the met4 transcription factor by ubiquitin-dependent degradation and
594 inhibition of promoter recruitment. *Mol Cell*, 10, 69-80.
- 595 LAXMAN, S., SUTTER, B. M., WU, X., KUMAR, S., GUO, X., TRUDGIAN, D. C.,
596 MIRZAEI, H. & TU, B. P. 2013. Sulfur amino acids regulate translational capacity and
597 metabolic homeostasis through modulation of tRNA thiolation. *Cell*, 154, 416-29.
- 598 LIU, K., SANTOS, D. A., HUSSMANN, J. A., SUTTER, B. M., WANG, Y., WEISSMAN, J. S.
599 & TU, B. P. Regulation of translation by 18S rRNA methylation multiplicity.
- 600 LJUNGDAHL, P. O. & DAIGNAN-FORNIER, B. 2012. Regulation of amino acid, nucleotide,
601 and phosphate metabolism in *Saccharomyces cerevisiae*. *Genetics*, 190, 885-929.
- 602 LONGTINE, M. S., MCKENZIE, A., 3RD, DEMARINI, D. J., SHAH, N. G., WACH, A.,
603 BRACHAT, A., PHILIPPSEN, P. & PRINGLE, J. R. 1998. Additional modules for
604 versatile and economical PCR-based gene deletion and modification in *Saccharomyces*
605 *cerevisiae*. *Yeast*, 14, 953-61.
- 606 MENANT, A., BAUDOUIN-CORNU, P., PEYRAUD, C., TYERS, M. & THOMAS, D. 2006.
607 Determinants of the ubiquitin-mediated degradation of the Met4 transcription factor. *J*
608 *Biol Chem*, 281, 11744-54.
- 609 MILLER, A. W., BEFORT, C., KERR, E. O. & DUNHAM, M. J. 2013. Design and use of
610 multiplexed chemostat arrays. *JoVE (Journal of Visualized Experiments)*, e50262.
- 611 PENNINCKX, M. 2000. A short review on the role of glutathione in the response of yeasts to
612 nutritional, environmental, and oxidative stresses. *Enzyme Microb Technol*, 26, 737-742.
- 613 PETROSKI, M. D. & DESHAIES, R. J. 2005. In vitro reconstitution of SCF substrate
614 ubiquitination with purified proteins. *Methods Enzymol*, 398, 143-58.
- 615 POMPELLA, A., VISVIKIS, A., PAOLICCHI, A., DE TATA, V. & CASINI, A. F. 2003. The
616 changing faces of glutathione, a cellular protagonist. *Biochem Pharmacol*, 66, 1499-503.
- 617 REITSMA, J. M., LIU, X., REICHERMEIER, K. M., MORADIAN, A., SWEREDOSKI, M. J.,
618 HESS, S. & DESHAIES, R. J. 2017. Composition and regulation of the cellular
619 repertoire of SCF ubiquitin ligases. *Cell*, 171, 1326-1339. e14.
- 620 ROUILLON, A., BARBEY, R., PATTON, E. E., TYERS, M. & THOMAS, D. 2000. Feedback-
621 regulated degradation of the transcriptional activator Met4 is triggered by the SCF(Met30
622)complex. *EMBO J*, 19, 282-94.

- 623 SADHU, M. J., MORESCO, J. J., ZIMMER, A. D., YATES, J. R., 3RD & RINE, J. 2014.
624 Multiple inputs control sulfur-containing amino acid synthesis in *Saccharomyces*
625 *cerevisiae*. *Mol Biol Cell*, 25, 1653-65.
- 626 SU, N. Y., FLICK, K. & KAISER, P. 2005. The F-box protein Met30 is required for multiple
627 steps in the budding yeast cell cycle. *Mol Cell Biol*, 25, 3875-85.
- 628 SU, N. Y., OUNI, I., PAPAGIANNIS, C. V. & KAISER, P. 2008. A dominant suppressor
629 mutation of the met30 cell cycle defect suggests regulation of the *Saccharomyces*
630 *cerevisiae* Met4-Cbf1 transcription complex by Met32. *J Biol Chem*, 283, 11615-24.
- 631 SUTTER, B. M., WU, X., LAXMAN, S. & TU, B. P. 2013. Methionine inhibits autophagy and
632 promotes growth by inducing the SAM-responsive methylation of PP2A. *Cell*, 154, 403-
633 15.
- 634 SUZUKI, T., MURAMATSU, A., SAITO, R., ISO, T., SHIBATA, T., KUWATA, K.,
635 KAWAGUCHI, S. I., IWAWAKI, T., ADACHI, S., SUDA, H., MORITA, M.,
636 UCHIDA, K., BAIRD, L. & YAMAMOTO, M. 2019. Molecular Mechanism of Cellular
637 Oxidative Stress Sensing by Keap1. *Cell Rep*, 28, 746-758 e4.
- 638 THOMAS, D., KURAS, L., BARBEY, R., CHEREST, H., BLAISEAU, P. L. & SURDIN-
639 KERJAN, Y. 1995. Met30p, a yeast transcriptional inhibitor that responds to S-
640 adenosylmethionine, is an essential protein with WD40 repeats. *Mol Cell Biol*, 15, 6526-
641 34.
- 642 TU, B. P., MOHLER, R. E., LIU, J. C., DOMBEK, K. M., YOUNG, E. T., SYNOVEC, R. E. &
643 MCKNIGHT, S. L. 2007. Cyclic changes in metabolic state during the life of a yeast cell.
644 *Proc Natl Acad Sci U S A*, 104, 16886-91.
- 645 VAN DIJKEN, J. P., BAUER, J., BRAMBILLA, L., DUBOC, P., FRANCOIS, J. M.,
646 GANCEDO, C., GIUSEPPIN, M. L., HEIJNEN, J. J., HOARE, M., LANGE, H. C.,
647 MADDEN, E. A., NIEDERBERGER, P., NIELSEN, J., PARROU, J. L., PETIT, T.,
648 PORRO, D., REUSS, M., VAN RIEL, N., RIZZI, M., STEENSMA, H. Y., VERRIPS, C.
649 T., VINDELOV, J. & PRONK, J. T. 2000. An interlaboratory comparison of
650 physiological and genetic properties of four *Saccharomyces cerevisiae* strains. *Enzyme*
651 *Microb Technol*, 26, 706-714.
- 652 WU, G., FANG, Y. Z., YANG, S., LUPTON, J. R. & TURNER, N. D. 2004. Glutathione
653 metabolism and its implications for health. *J Nutr*, 134, 489-92.
- 654 WU, X. & TU, B. P. 2011. Selective regulation of autophagy by the Iml1-Npr2-Npr3 complex in
655 the absence of nitrogen starvation. *Mol Biol Cell*, 22, 4124-33.
- 656 YAMAMOTO, M., KENSLER, T. W. & MOTOHASHI, H. 2018. The KEAP1-NRF2 System: a
657 Thiol-Based Sensor-Effector Apparatus for Maintaining Redox Homeostasis. *Physiol*
658 *Rev*, 98, 1169-1203.

- 659 YANG, Y. S., KATO, M., WU, X., LITSIOS, A., SUTTER, B. M., WANG, Y., HSU, C. H.,
660 WOOD, N. E., LEMOFF, A., MIRZAEI, H., HEINEMANN, M. & TU, B. P. 2019.
661 Yeast Ataxin-2 Forms an Intracellular Condensate Required for the Inhibition of TORC1
662 Signaling during Respiratory Growth. *Cell*, 177, 697-710 e17.
- 663 YE, C., SUTTER, B. M., WANG, Y., KUANG, Z. & TU, B. P. 2017. A Metabolic Function for
664 Phospholipid and Histone Methylation. *Mol Cell*, 66, 180-193 e8.
- 665 YE, C., SUTTER, B. M., WANG, Y., KUANG, Z., ZHAO, X., YU, Y. & TU, B. P. 2019.
666 Demethylation of the Protein Phosphatase PP2A Promotes Demethylation of Histones to
667 Enable Their Function as a Methyl Group Sink. *Mol Cell*, 73, 1115-1126 e6.
- 668 YEN, J. L., FLICK, K., PAPAGIANNIS, C. V., MATHUR, R., TYRRELL, A., OUNI, I.,
669 KAAKE, R. M., HUANG, L. & KAISER, P. 2012. Signal-induced disassembly of the
670 SCF ubiquitin ligase complex by Cdc48/p97. *Mol Cell*, 48, 288-97.
- 671 YEN, J. L., SU, N. Y. & KAISER, P. 2005. The yeast ubiquitin ligase SCFMet30 regulates
672 heavy metal response. *Mol Biol Cell*, 16, 1872-82.
673
674

675 **FIGURE LEGENDS**

676

677 **Figure 1. Met30 and Met4 response to sulfur starvation and repletion under respiratory**
678 **growth conditions.**

679 (A) Western blot analysis of a time course performed with yeast containing endogenously tagged
680 Met30 and Met4 that were cultured in rich lactate media (Rich) overnight to mid log phase before
681 switching cells to sulfur-free lactate media (–sulfur) for 1 h, followed by the addition of a mix of
682 the sulfur containing metabolites methionine, homocysteine, and cysteine at 0.5 mM each
683 (+Met/Cys/Hcy).

684 (B) Expression of *MET* gene transcript levels was assessed by qPCR over the time course shown
685 in (A). Data are presented as mean and SEM of technical triplicates.

686 (C) Levels of key sulfur metabolites were measured over the same time course as in (A) and (B),
687 as determined by LC-MS/MS. Data represent the mean and SD of two biological replicates.

688 (D) *met6Δ* or *str3Δ* strains were grown in “Rich” YPL and switched to “–sulfur” SFL for 1 h to
689 induce sulfur starvation before the addition of either 0.5 mM homocysteine (+HCY), 0.5 mM
690 methionine (+MET), or 0.5 mM cysteine (+CYS).

691 (E) Simplified diagram of the sulfur metabolic pathway in yeast.

692

693 **Figure 2. Met30 cysteine residues become oxidized during sulfur starvation.**

694 (A) Schematic of Met30 protein architecture and cysteine residue location.

695 (B) Western blot analysis of Met30 cysteine redox state in lactate media as determined by
696 methoxy-PEG-maleimide (mPEG2K-mal) modification of reduced protein thiols. For every
697 reduced cysteine thiol in a protein, mPEG2K-mal adds ~ 2 kDa in apparent molecular weight.

698 (C) Same Western blot analysis as in (B), except that yeast were cultured in sulfur-free glucose
699 media (SFD) for 3 h before the addition of 0.5 mM each of the sulfur metabolites homocysteine,
700 methionine, and cysteine (+Met/Cys/Hcy).

701 (D) Yeast were subjected to the same rich to –sulfur media switch as in (B), except that following
702 the 15 min time point, 5 mM DTT was added to the culture for 15 min and Met30 cysteine residue
703 redox state and Met4 ubiquitination were assessed by Western blot.

704

705 **Figure 3. Met30 cysteine point mutants display dysregulated sulfur sensing.**

706 (A) Western blot analysis of Met30 cysteine redox state and Met4 ubiquitination status in WT and
707 two cysteine to serine mutants, C414S and C614/616/622/630S.

708 (B) *MET* gene transcript levels over the same time course as (A) for the three strains, as assessed
709 by qPCR. Data are presented as mean and SEM of technical triplicates.

710 (C) Growth curves of the three yeast strains used in (A) and (B) in sulfur-rich YPL media or –sulfur
711 SFL media supplemented with 0.2 mM homocysteine. Cells were grown to mid-log phase in YPL
712 media before pelleting, washing with water, and back-diluting yeast into the two media conditions.
713 Data represent mean and SD of technical triplicates.

714

715 **Figure 4. Met30 cysteine oxidation disrupts ubiquitination and reduces binding to Met4 *in***
716 ***vitro*.**

717 (A) Schematic for the large-scale SCF^{Met30-Flag} immunopurification from rich high sulfur (YPL)
718 and –sulfur (SFL) conditions for use in *in vitro* ubiquitination or binding assays with recombinant
719 Met4 protein.

720 (B) Western blot analysis of Met4 *in vitro* ubiquitination by SCF^{Met30-Flag} immunopurifications
721 from cells cultured in sulfur-replete rich media. Cryomilled YPL yeast powder was divided evenly
722 for two Flag IPs performed identically with the exception that one was done in the presence of 1
723 mM DTT (+DTT) and the other was performed without reducing agent present (–DTT). To test if
724 the addition of reducing agent could rescue the activity of the “–DTT” IP, a small aliquot of the
725 “–DTT” SCF^{Met30-Flag} complex was transferred to a new tube and was treated briefly with 5 mM
726 TCEP while the *in vitro* ubiquitination reaction was set up (–DTT/+TCEP). The first three lanes
727 are negative control reactions performed either without SCF^{Met30-Flag} IP, recombinant Met4, or
728 ubiquitin.

729 (C) The same Western blot analysis of Met4 *in vitro* ubiquitination as in (B), except that the
730 SCF^{Met30-Flag} complex was produced from –sulfur SFL cells.

731 (D) Western blot analysis of the Met4 binding assay illustrated in (A). Rich and –sulfur lysate
732 were both split three ways, and lysate with 1 mM DTT (+DTT), 1 mM diamide (+Diamide), or
733 control (–DTT) were incubated with anti-Flag magnetic beads to isolate Met30-Flag complex. The
734 Met30-Flag bound beads from each condition were then split in half and distributed into tubes
735 containing IP buffer ± 1 mM DTT and purified recombinant Met4. The mixture was allowed to
736 incubate for 2 h before the beads were washed, boiled in sample buffer, and bound proteins were
737 separated on SDS-PAGE gels and Western blots were performed for both Met30 and Met4.

738

739 **Figure 5. Model for sulfur-sensing and *MET* gene regulation by the SCF^{Met30} E3 ligase.**

740 In conditions of high sulfur metabolite levels, cysteine residues in the WD-40 repeat region of
741 Met30 are reduced, allowing Met30 to bind and facilitate ubiquitination of Met4 in order to
742 negatively regulate the transcriptional activation of the *MET* regulon. Upon sulfur starvation,
743 Met30 cysteine residues become oxidized, resulting in conformational changes in Met30 that allow
744 Met4 to be released from the SCF^{Met30} complex, deubiquitinated, and transcriptionally active.

745

746 **SUPPLEMENTAL FIGURE LEGENDS**

747

748 **Figure S1. Characterization of the faster-migrating proteoform of Met30.**

749 (A) Western blot of yeast treated with 200 $\mu\text{g/ml}$ cycloheximide during sulfur starvation
750 demonstrates that production of the faster-migrating proteoform is dependent on new translation.

751 (B) The faster-migrating proteoform persists after rescue from sulfur starvation when treated with
752 a proteasome inhibitor. Cells were starved of sulfur for 3 h to accumulate the faster-migrating
753 proteoform, and then sulfur metabolites were added back concomitantly with MG132 (50 μM).

754 (C) The faster-migrating proteoform of Met30 is dependent on Met4. The *met4* Δ yeast strain does
755 not produce the second proteoform of Met30 when starved of sulfur.

756 (D) Western blot analysis of strains expressing either wild type Met30, Met30 Δ 1-20aa, or Met30
757 M30/35/36A. Yeast cells harboring the N-terminal deletion of the first twenty amino acids of
758 Met30 (which contain the first three methionine residues) or have the subsequent three methionine
759 residues (M30/35/36) mutated to alanine do not create faster-migrating proteoforms.

760 (E) Met30(Δ 1-20aa) and Met30(M30/35/36A) strains do not exhibit any growth phenotypes in
761 $-\text{sulfur}$ glucose media with or without supplemented methionine. There are also no defects in
762 growth rate following repletion of methionine. Data represent mean and SD of technical triplicates.

763

764 **Figure S2. Identification of key cysteine residues in Met30 involved specifically in sulfur**
765 **amino acid sensing.**

766 (A) Schematic of Met30 protein architecture and cysteine residue location.

767 (B) Western blot analysis of various Met30 cysteine point mutants and Met4 ubiquitination status
768 in rich and $-\text{sulfur}$ media.

769 (C) Western blot analysis of Met30 cysteine redox state and Met4 ubiquitination status in WT and
770 two cysteine to serine mutants, C414S and C614/616/622/630S, following treatment with 500 μM
771 CdCl_2 .

772

773 **Figure S3. SCF^{Met30-Flag} IP/*in vitro* ubiquitination assay demonstrating the dependence of**
774 **reducing agent in the IP on SCF^{Met30} E3 ligase activity.**

775 (A) Initial IPs for SCF^{Met30-Flag} complex were performed in the presence of 1 mM DTT prior to
776 Flag peptide elution and concentration. No DTT was used in the *in vitro* ubiquitination assay itself,
777 yet the E3 ligase activities for the E3 complex were indistinguishable between complex isolated
778 from high sulfur versus low sulfur cells.

779 (B) The same IP/*in vitro* assay as in (A), with the sole exception that DTT was not included during
780 the IP and wash steps.

781 (C) Silver stains of immunopurified SCF^{Met30-Flag} complex isolated from rich and $-\text{sulfur}$ cells
782 prepared in the presence or absence of DTT used in Figures 4B and C.

783 (D) Western blot of Cdc53 amounts from immunopurified SCF^{Met30-Flag} complex shown in S2C
784 and used in Figures 4B and C. We speculate the reduced Cdc53 abundance in the $-\text{sulfur}$, $-\text{DTT}$
785 IP is the result of the canonical regulation of SCF E3 ligases, which causes reduced association

786 between Skp1/F-box heterodimers to the Cdc53 scaffold when binding between the F-box and its
787 substrate is reduced.

788

789 **Figure S4. SCF^{Met30-Flag} IP/*in vitro* ubiquitination assay using Met30 cysteine point mutants**

790 (A) *In vitro* ubiquitination assays were carried out as described in Figure 4B with cell lysate
791 powder from WT, C414S, and C614/616/622/630S Met30 strains grown in rich media. The heavier
792 loading of the C414S mutant is likely due to a difference in cryomill lysis efficiency, and is not a
793 difference in the amount of starting material used.

794 (B) Met4 binding was assessed in the C414S and C614/616/622/630S mutants as described in
795 Figure 4D using cell lysate powder from cells grown in rich media. The fold change in Met4
796 binding in the presence and absence of DTT was quantified for each strain and for each Met30
797 immunopurification condition using ImageJ (version 1.53).

798 **Table S1. Strains used in this study.**

BACKGROUND	GENOTYPE	SOURCE
CEN.PK	MATa	(van Dijken et al., 2000)
CEN.PK	MAT α	(van Dijken et al., 2000)
CEN.PK	MATa; MET30-FLAG::KanMX	This study
CEN.PK	MATa; MET30-FLAG::KanMX MET4-HA::Hyg	This study
CEN.PK	MATa; MET30-FLAG::KanMX MET4-HA::Hyg met6 Δ ::Nat	This study
CEN.PK	MATa; MET30-FLAG::KanMX MET4-HA::Hyg str3 Δ ::Nat	This study
CEN.PK	MATa; met30::MET30-C414S-FLAG::KanMX MET4-HA::Hyg	This study
CEN.PK	MATa; met30::MET30-C614/616/622/630S- FLAG::KanMX MET4-HA::Hyg	This study
CEN.PK	MATa; met30 Δ ::Phleo HO::MET30-FLAG::Nat MET4-HA::Hyg	This study
CEN.PK	MATa; met30 Δ ::Phleo HO::MET30 Δ aa1-20- FLAG::Nat Met4-HA::Hyg	This study
CEN.PK	MATa; met30 Δ ::Phleo HO::MET30-M30/35/36A- FLAG::Nat Met4-HA::Hyg	This study
CEN.PK	MATa; MET30-FLAG::KanMX MET4-HA::Hyg pdr5 Δ ::Nat	This study
CEN.PK	MATa; met4 Δ ::KanMX MET30-FLAG::Hyg	This study
CEN.PK	MATa; cup1p-6xHis-TEV-UBA1::Hyg	This study
CEN.PK	MATa; met30::MET30-C201S-FLAG::KanMX MET4-HA::Hyg	This study
CEN.PK	MATa; met30::MET30-C374S-FLAG::KanMX MET4-HA::Hyg	This study
CEN.PK	MATa; met30::MET30-C426S-FLAG::KanMX MET4-HA::Hyg	This study
CEN.PK	MATa; met30::MET30-C436S-FLAG::KanMX MET4-HA::Hyg	This study
CEN.PK	MATa; met30::MET30-C439S-FLAG::KanMX MET4-HA::Hyg	This study
CEN.PK	MATa; met30::MET30-C455S-FLAG::KanMX MET4-HA::Hyg	This study
CEN.PK	MATa; met30::MET30-C528S-FLAG::KanMX MET4-HA::Hyg	This study
CEN.PK	MATa; met30::MET30-C544S-FLAG::KanMX MET4-HA::Hyg	This study
CEN.PK	MATa; met30::MET30-C584S-FLAG::KanMX MET4-HA::Hyg	This study

CEN.PK	MATa; met30::MET30-C614S-FLAG::KanMX MET4-HA::Hyg	This study
CEN.PK	MATa; met30::MET30-C616S-FLAG::KanMX MET4-HA::Hyg	This study
CEN.PK	MATa; met30::MET30-C584/622S-FLAG::KanMX MET4-HA::Hyg	This study
CEN.PK	MATa; met30::MET30-C630S-FLAG::KanMX MET4-HA::Hyg	This study

799

800 **Table S2. Recipe for sulfur-free media.**

salts (g L⁻¹)	
CaCl ₂ •2H ₂ O	0.1
NaCl	0.1
MgCl ₂ •6H ₂ O	0.412
NH ₄ Cl	4.05
KH ₂ PO ₄	1
metals (mg L⁻¹)	
boric acid	0.5
CuCl ₂ •2H ₂ O	0.0273
KI	0.1
FeCl ₃ •6H ₂ O	0.2
MnCl ₂ •4H ₂ O	0.4684
Na ₂ MoO ₄ •2H ₂ O	0.2
ZnCl ₂ •H ₂ O	0.1895
vitamins (mg L⁻¹)	
biotin	0.002
calcium pantothenate	0.4
folic acid	0.002
inositol	2
niacin	0.4
4-aminobenzoic acid	0.2
pyridoxine HCl	0.4
riboflavin	0.2
thiamine-HCl	0.4

801

802 Recipes are derived from (Miller et al., 2013).

Figure 1

bioRxiv preprint doi: <https://doi.org/10.1101/2021.01.06.425657>; this version posted January 7, 2021. The copyright holder for this preprint (which was not certified by peer review) is the author/funder, who has granted bioRxiv a license to display the preprint in perpetuity. It is made available under aCC-BY 4.0 International license.

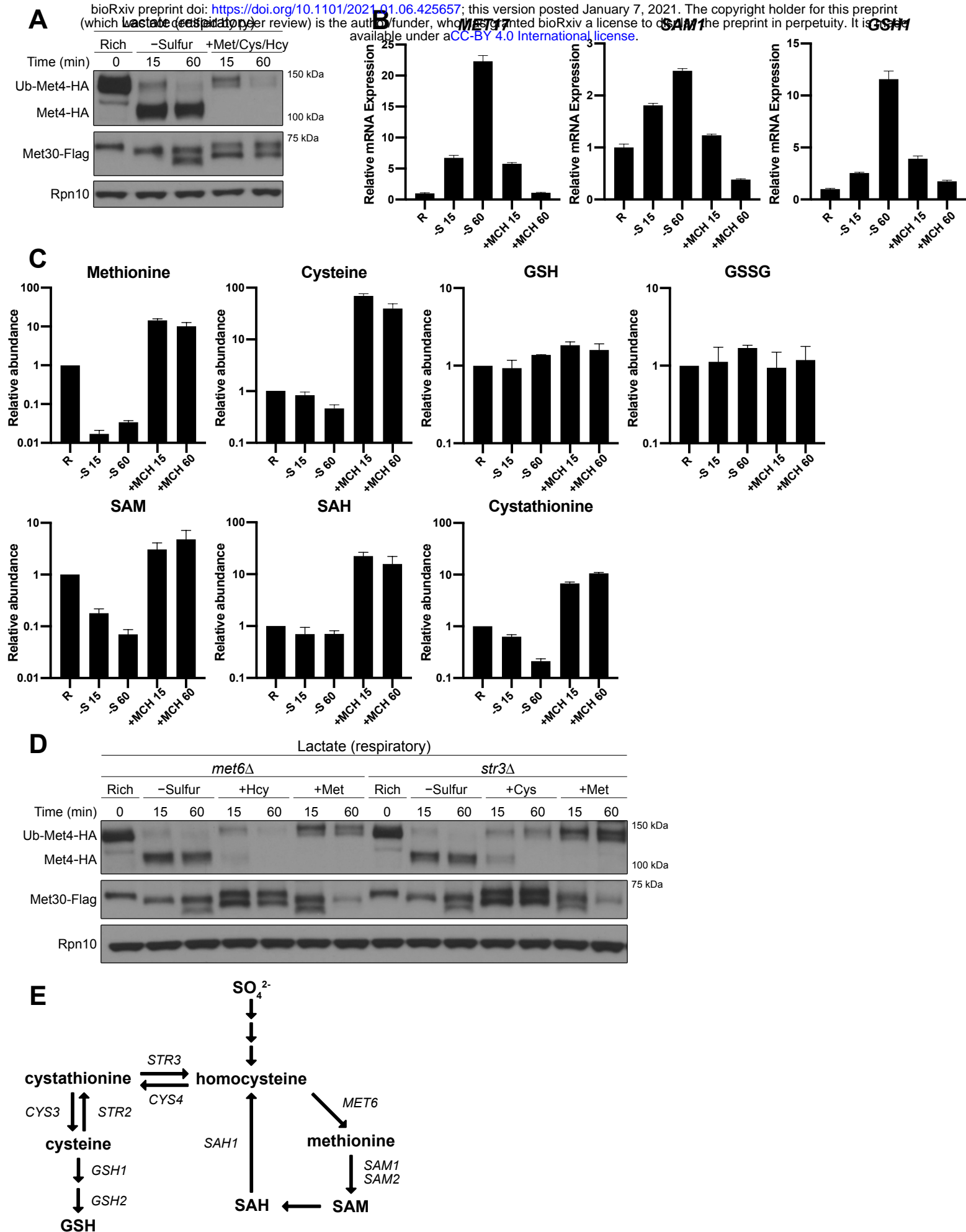
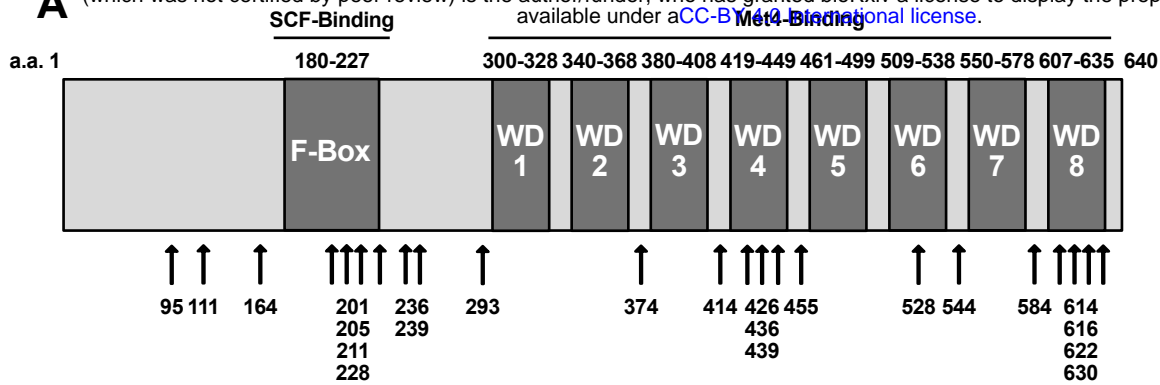


Figure 2

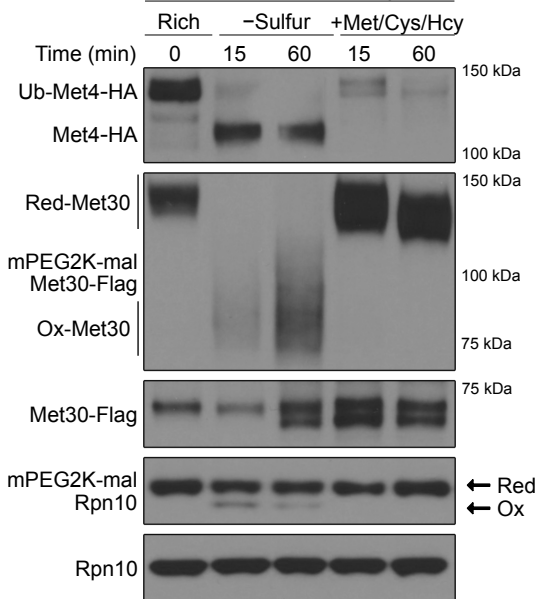
bioRxiv preprint doi: <https://doi.org/10.1101/2021.01.06.425657>; this version posted January 7, 2021. The copyright holder for this preprint (which was not certified by peer review) is the author/funder, who has granted bioRxiv a license to display the preprint in perpetuity. It is made available under aCC-BY 4.0 International license.

A



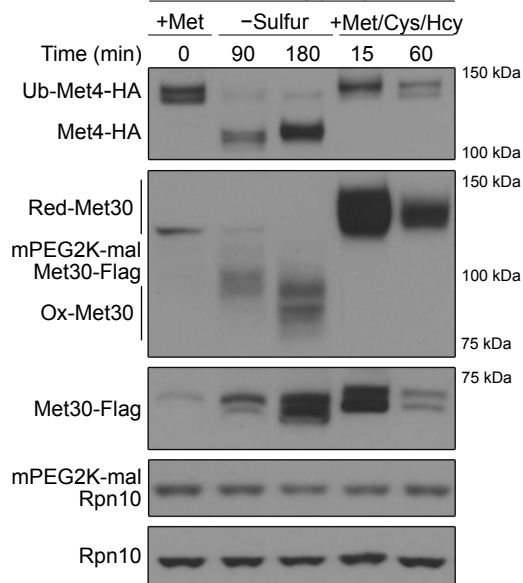
B

Lactate (respiratory)



C

Glucose (glycolytic)



D

Lactate (respiratory)

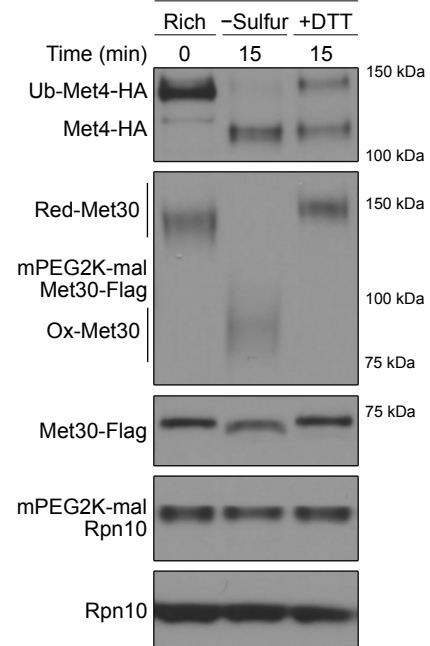


Figure 3

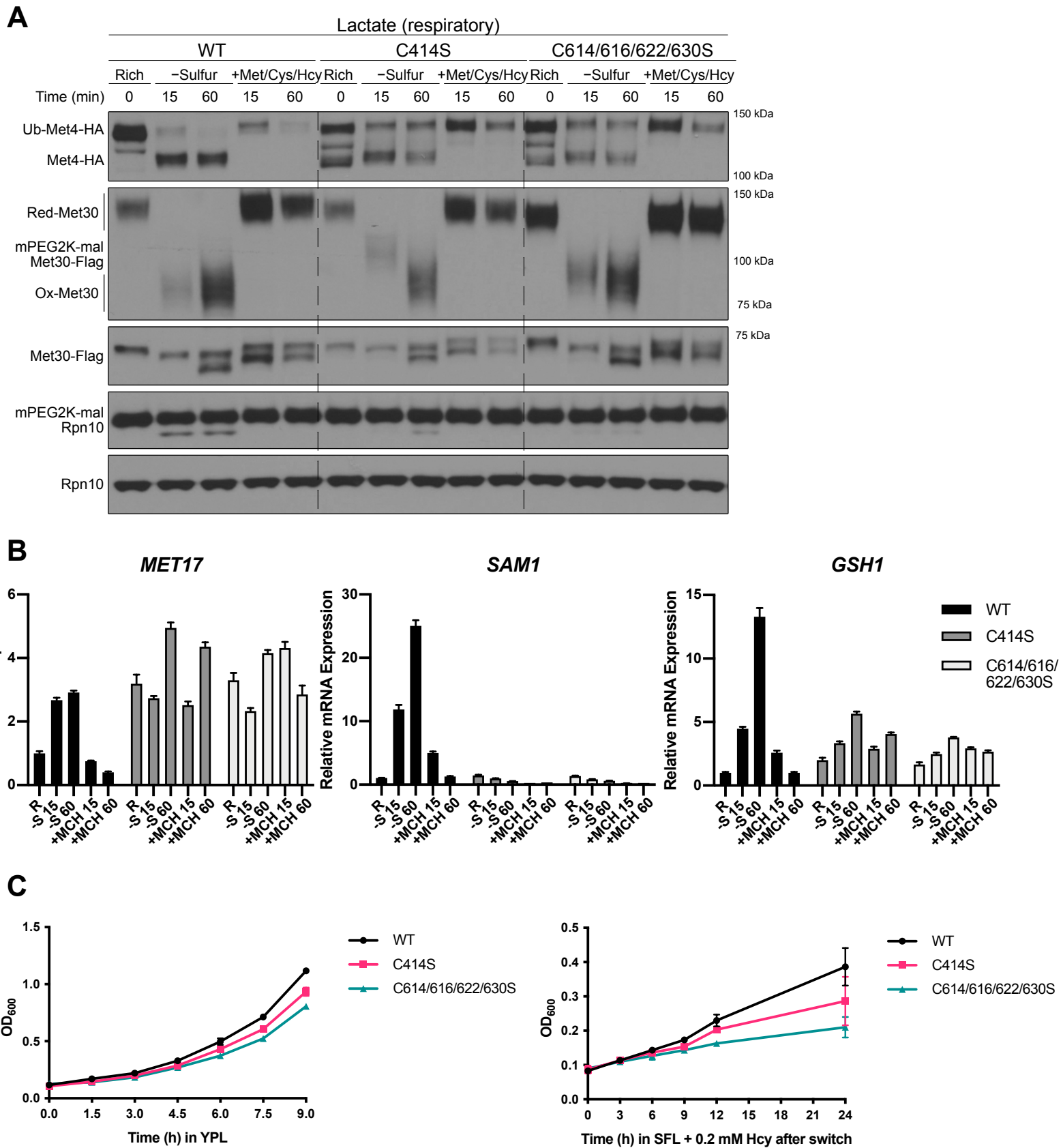
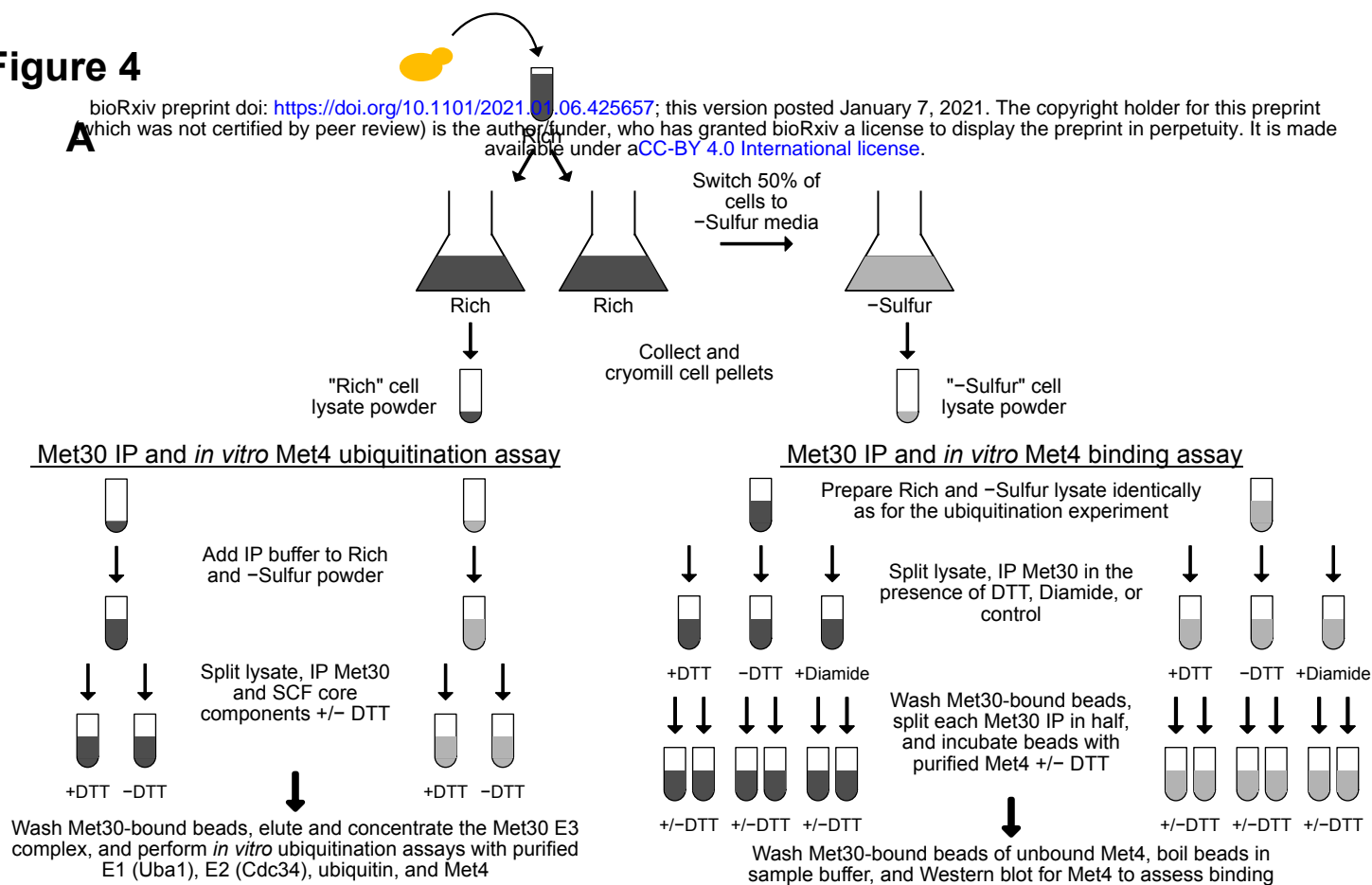


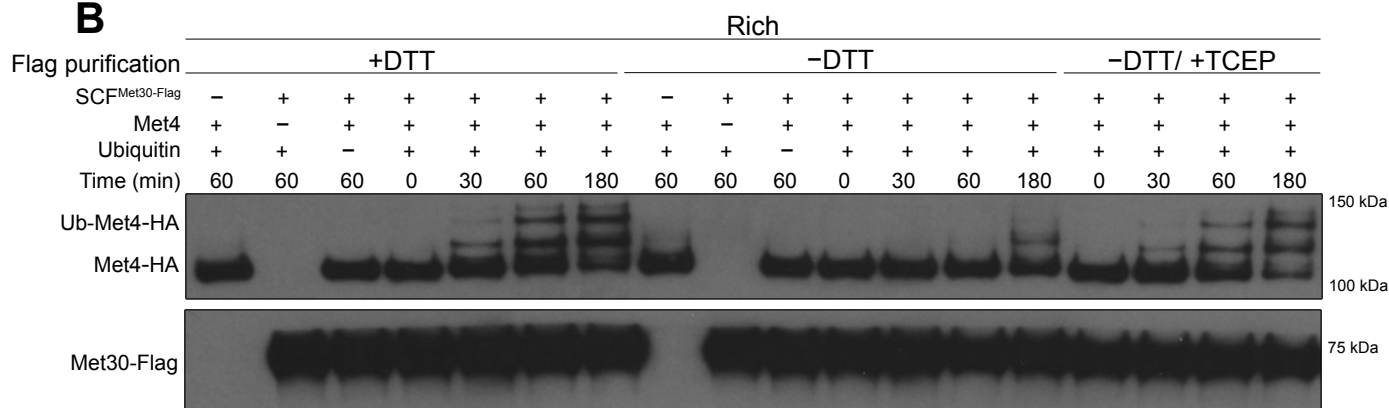
Figure 4

bioRxiv preprint doi: <https://doi.org/10.1101/2021.01.06.425657>; this version posted January 7, 2021. The copyright holder for this preprint (which was not certified by peer review) is the author/funder, who has granted bioRxiv a license to display the preprint in perpetuity. It is made available under aCC-BY 4.0 International license.

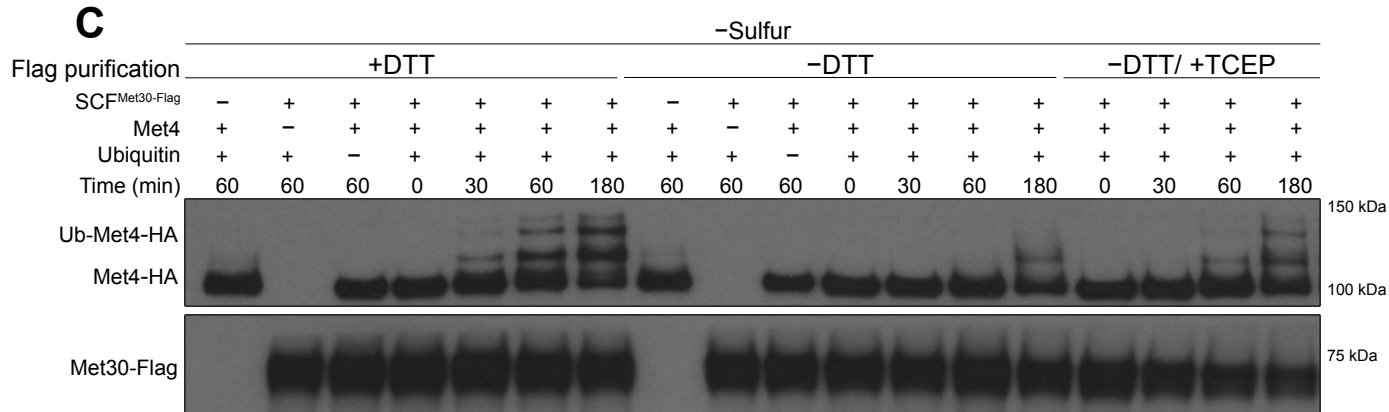
A



B



C



D

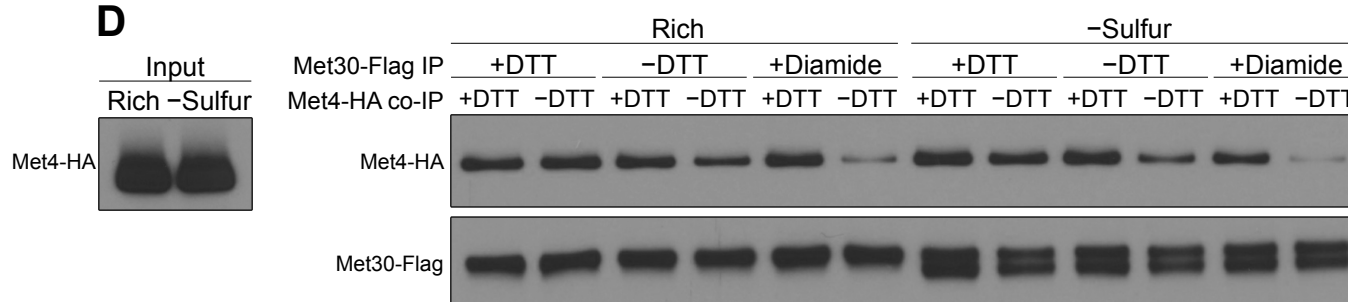


Figure 5

bioRxiv preprint doi: <https://doi.org/10.1101/2021.01.06.425657>; this version posted January 7, 2021. The copyright holder for this preprint (which was not certified by peer review) is the author/funder, who has granted bioRxiv a license to display the preprint in perpetuity. It is made available under aCC-BY 4.0 International license.

A

High sulfur metabolite levels

Low sulfur metabolite levels

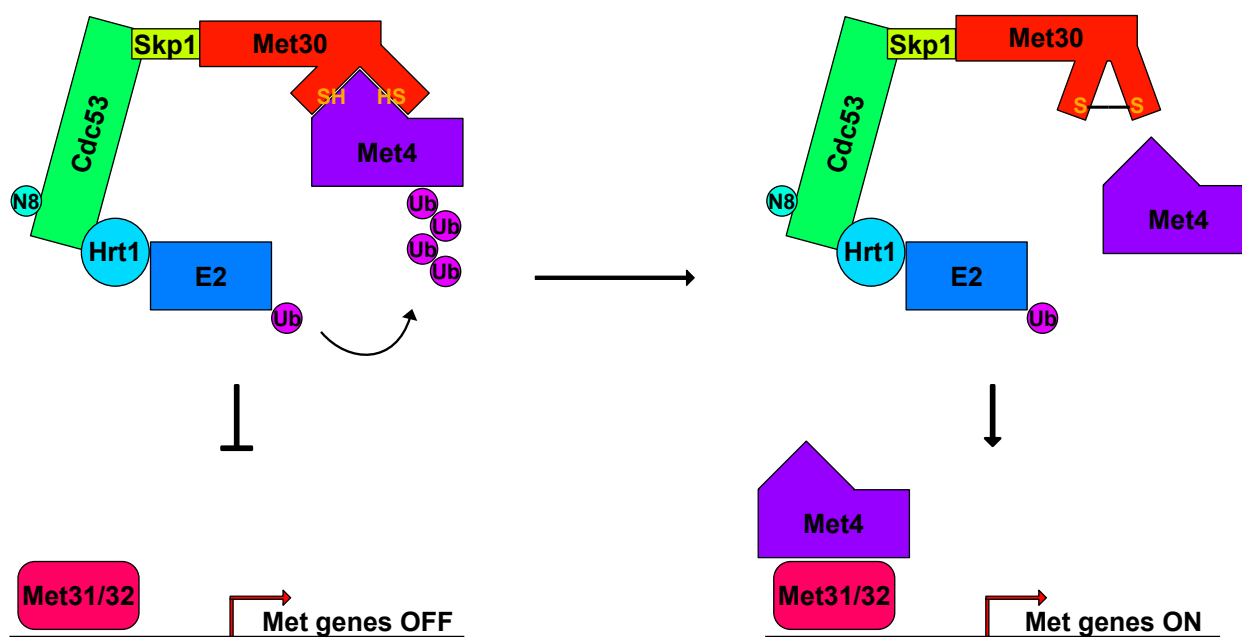


Figure S1

bioRxiv preprint doi: <https://doi.org/10.1101/2021.01.06.425657>; this version posted January 7, 2021. The copyright holder for this preprint (which was not certified by peer review) is the author/funder, who has granted bioRxiv a license to display the preprint in perpetuity. It is made available under aCC-BY 4.0 International license.

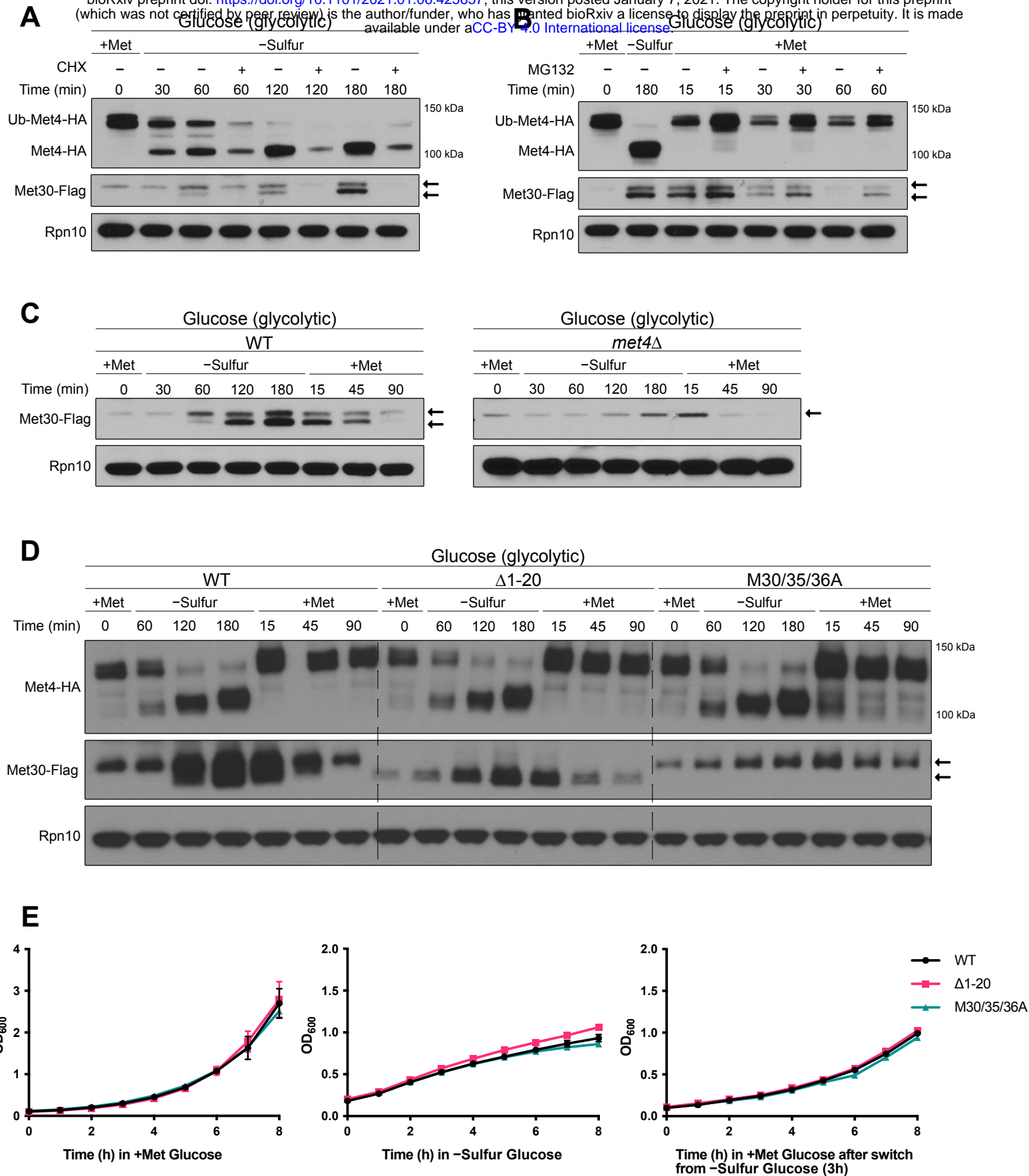


Figure S2

A bioRxiv preprint doi: <https://doi.org/10.1101/2021.01.06.425657>; this version posted January 7, 2021. The copyright holder for this preprint (which was not certified by peer review) is the author/funder, who has granted bioRxiv a license to display the preprint in perpetuity. It is made available under a [CC-BY 4.0 International license](https://creativecommons.org/licenses/by/4.0/).

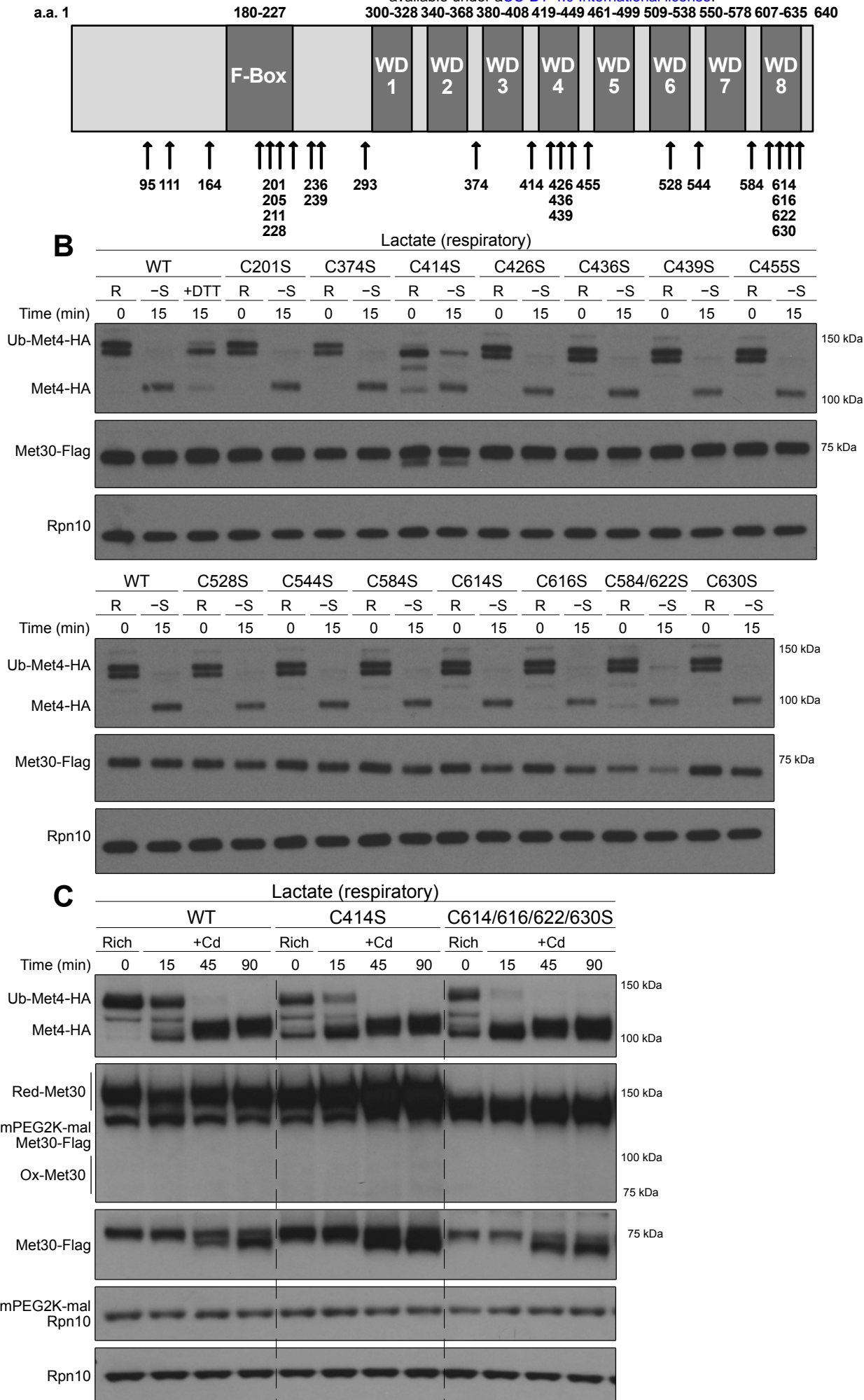


Figure S3

bioRxiv preprint doi: <https://doi.org/10.1101/2021.01.06.425657>; this version posted January 7, 2021. The copyright holder for this preprint (which was not certified by peer review) is the author/funder, who has granted bioRxiv a license to display the preprint in perpetuity. It is made available under aCC-BY 4.0 International license.

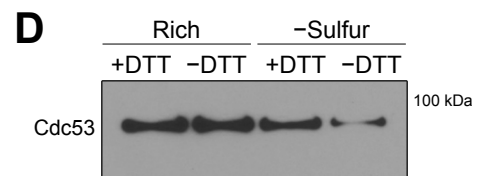
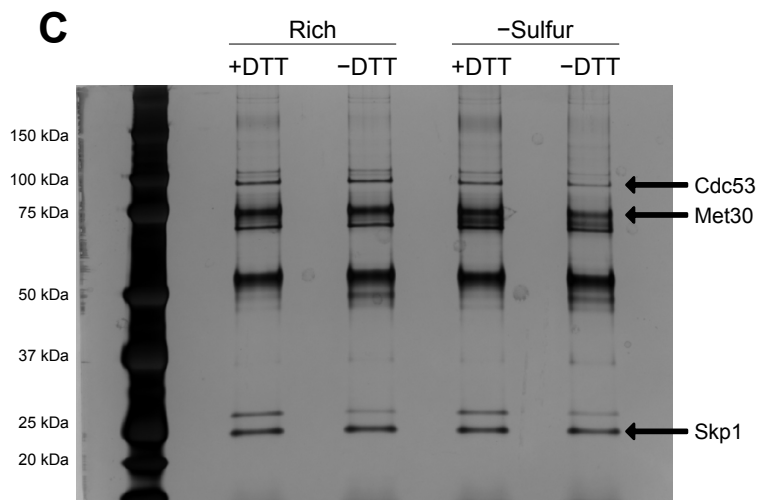
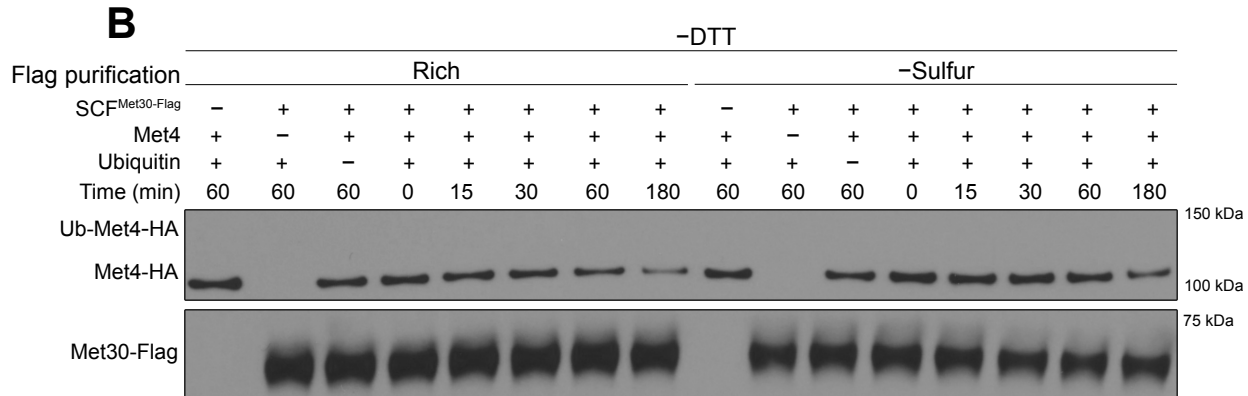
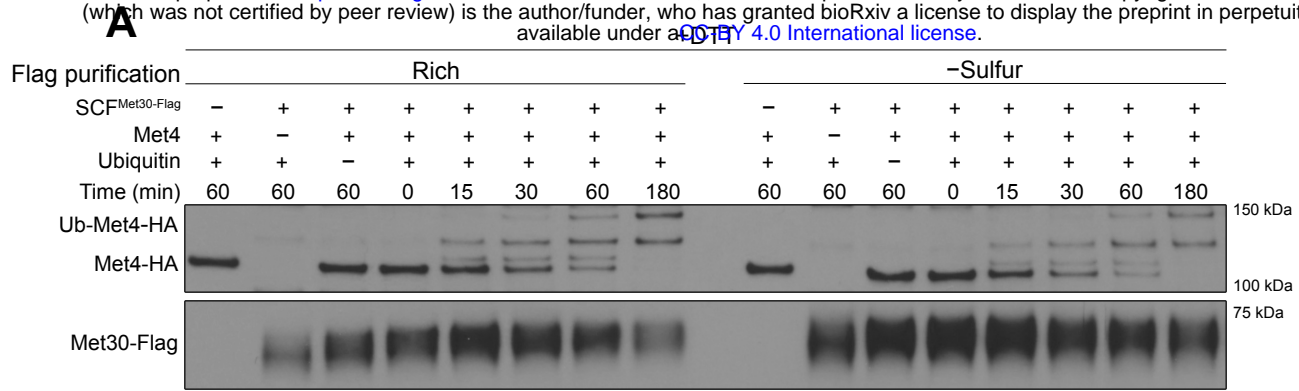


Figure S4

bioRxiv preprint doi: <https://doi.org/10.1101/2021.01.06.425657>; this version posted January 7, 2021. The copyright holder for this preprint (which was not certified by peer review) is the author/funder, who has granted bioRxiv a license to display the preprint in perpetuity. It is made available under aCC-BY 4.0 International license.

